

Geometric analysis of a reaction-diffusion equation with nonlocal inhibition
by Joseph Boyd Raquepas

A thesis submitted in partial fulfillment of the requirements for the degree of Doctor of Philosophy in Mathematics .
Montana State University
© Copyright by Joseph Boyd Raquepas (1997)

Abstract:
Presented are geometric results for a reaction-diffusion equation with nonlocal, inhibitory feedback. The equation corresponds to the limiting equation on the slow manifold for a singularly perturbed activator-inhibitor system. The existence of solutions and a global attractor is established using standard results of linear and nonlinear semigroup theory. The bifurcation of equilibria is studied and family of secondary bifurcations is demonstrated, by means of Lyapunov-Schmidt reduction. The -existence of an inertial manifold is verified as well as a family of approximate inertial manifolds. Evidence for the qualitative structure of the global attractor is provided using approximate inertial manifolds and simulations based on standard numerical methods.

GEOMETRIC ANALYSIS OF A REACTION-DIFFUSION EQUATION WITH NONLOCAL INHIBITION

by

Joseph Boyd Raquepas

A thesis submitted in partial fulfillment
of the requirements for the degree

of

Doctor of Philosophy

in

Mathematics

MONTANA STATE UNIVERSITY
Bozeman, Montana

July 1997

D378
R1824

APPROVAL

of a thesis submitted by

Joseph Boyd Raquepas

This thesis has been read by each member of the thesis committee and has been found to be satisfactory regarding content, English usage, format, citations, bibliographic style, and consistency, and is ready for submission to the College of Graduate Studies.

7-16-97
Date

Jack D. Dockery
Chairperson, Graduate Committee

Approved for the Major Department

7/16/97
Date

John Lund
Head, Mathematics

Approved for the College of Graduate Studies

7/18/97
Date

Robert Brown
Graduate Dean

STATEMENT OF PERMISSION TO USE

In presenting this thesis in partial fulfillment for a doctoral degree at Montana State University, I agree that the Library shall make it available to borrowers under rules of the Library. I further agree that copying of this thesis is allowable only for scholarly purposes, consistent with "fair use" as prescribed in the U. S. Copyright Law. Requests for extensive copying or reproduction of this thesis should be referred to University Microfilms International, 300 North Zeeb Road, Ann Arbor, Michigan 48106, to whom I have granted "the exclusive right to reproduce and distribute copies of the dissertation for sale in and from microform or electronic format, along with the right to reproduce and distribute my abstract in any format in whole or in part."

Signature Joseph Boyd Ragsdale

Date 7-16-97

TABLE OF CONTENTS

Page

LIST OF TABLES vi

LIST OF FIGURES vii

ABSTRACT ix

1. INTRODUCTION 1

2. PRELIMINARY RESULTS 6

Introduction 6
Operator Theory and Function Spaces 7
Existence of Solutions and the Global Attractor 11

3. BIFURCATION RESULTS 19

Introduction 19
Bifurcations from Simple Eigenvalues 21
Bifurcations from the Zero Solution 25
Modal Bifurcations from the Zero Solution 26
Computation of the Local Solution Branch 27
Stability of the Bifurcating Solutions 30
Secondary Bifurcations: Lyapunov Schmidt Reduction 33
Bifurcations from the Non-zero Constant Solutions 41

4. INERTIAL MANIFOLDS 43

Introduction 43
Existence of an Inertial Manifold 44
Approximate Inertial Manifolds 49

5. APPROXIMATION OF THE ATTRACTOR 59

Introduction 59
Bifurcation Results 60

Approximation of the Connecting Orbits 69
Dynamics of the Inertial Forms 70
Numerical Computation of Connecting Orbits 74
Regions R_1 and R_2 77
Region R_3 78
Region R_4 80
Region R_5 80
Region R_6 87

6. CONCLUDING REMARKS 89

REFERENCES CITED 91

LIST OF TABLES

Table Page
1 Dimension estimates for $\mathcal{M}^s$ in $L^2(0,1)$. 51

LIST OF FIGURES

Figure		Page
1	Primary bifurcation curves for modes 0, 1, 2 and 3.	27
2	Local solution branch.	29
3	Mode 1 and 2 solutions. Steepening of transition layers occurs as $\epsilon \to 0$.	29
4	Modal bifurcations from zero and their local Morse index.	32
5	Bifurcation curve intersection point.	33
6	Bifurcation curves in local parameter coordinates.	38
7	Bifurcation diagram along path **A**.	38
8	Bifurcation curves for modes 2 and 3 : primary (solid), secondary (- -).	40
9	Bifurcation diagram for modes 2 and 3, $\rho = 0.01$: a and b modes (solid), mixed modes (- -).	40
10	Constant solution bifurcation curves.	42
11	Mode-one secondary bifurcation points: AUTO (o), AIM-0 (-.-), AIM-1 (solid), Γ_s (- -).	63
12	Mode-one residual errors at bifurcation points : AIM-0 (-.-), AIM-1 (-).	64
13	Bifurcation curves in the region $\mathcal{U}$.	66
14	γ-Bifurcation diagrams on path **A** for $\epsilon = 0.28$: constant solutions (solid), mode-one (- -), mixed modes (-.-).	66
15	γ-Bifurcation diagrams for $\epsilon = 0.28$: constant solutions (solid), mode-one (- -), mixed modes (-.-).	67
16	γ-Bifurcation diagrams for $\epsilon = 0.23$: constant solutions (solid), mode-one (- -), mixed modes (-.-).	68
17	Mixed mode solutions computed by AUTO: $\epsilon = 0.23$, $0.2 \leq \gamma \leq 0.87$.	69
18	Regions in parameter space.	70
19	Attractors for AIM-1.	71
20	Attractors for AIM-1 passing through R_5.	73
21	Attractor for R_2.	78
22	R_3 Connection from zero to m_1^+ : $\alpha = 1.25$, $\epsilon = 0.25$.	79
23	Equilibria and connections for R_3.	79
24	R_4 connection from zero to m_1^+ : $\alpha = 0.95$, $\epsilon = 0.25$.	81
25	R_4 connection from m_0^+ to m_1^+ : $\alpha = 0.95$, $\epsilon = 0.25$.	81
26	Equilibria and connections for R_4.	82
27	R_5 connection from zero to m_1^+ : $\alpha = 0.65$, $\epsilon = 0.25$.	82
28	Mixed mode solution $m_s^{(1)}$ and its principle eigenfunction: $\alpha = .65$, $\epsilon = 0.25$.	83
29	Connection from $m_s^{(1)}$ to m_1^+ : $\alpha = 0.65$, $\epsilon = 0.25$.	84
30	Connection from $m_s^{(1)}$ to m_0^+ : $\alpha = 0.65$, $\epsilon = 0.25$.	85

31 Connection from zero to $m_s^{(1)}$: $\alpha = 0.65$, $\epsilon = 0.25$. 85
32 Equilibria and connections for R_5. 86
33 Equilibria and connections for R_6. 87
34 Summary of equilibria and connections in $\mathcal{U}$. 88

ABSTRACT

Presented are geometric results for a reaction-diffusion equation with nonlocal, inhibitory feedback. The equation corresponds to the limiting equation on the slow manifold for a singularly perturbed activator-inhibitor system. The existence of solutions and a global attractor is established using standard results of linear and nonlinear semigroup theory. The bifurcation of equilibria is studied and family of secondary bifurcations is demonstrated, by means of Lyapunov-Schmidt reduction. The existence of an inertial manifold is verified as well as a family of approximate inertial manifolds. Evidence for the qualitative structure of the global attractor is provided using approximate inertial manifolds and simulations based on standard numerical methods.

CHAPTER 1

INTRODUCTION

In this thesis, we investigate the dynamics of the reaction-diffusion equation

$$u_t = \epsilon^2 u_{xx} + f(u) + \gamma \int_0^1 g(x,s)u(s)dx, \quad u_x(0,t) = u_x(1,t) = 0. \tag{1.1}$$

This equation corresponds to the flow on the slow manifold for the singularly perturbed reaction-diffusion system

$$u_t = \epsilon^2 u_{xx} + f(u) - w, \quad u_x(0,t) = u_x(1,t) = 0, \tag{1.2}$$

$$\delta w_t = D w_{xx} + \gamma u - w, \quad w_x(0,t) = w_x(1,t) = 0, \tag{1.3}$$

where $\delta \ll 1$. Equation (1.1) is obtained by formally setting $\delta = 0$ and using a Green's function to solve (1.3) for w as a function of u. Systems such as (1.2)-(1.3) arise frequently as mathematical models in biology, physiology, morphogenesis in embryology, and chemical systems to name a few. Many examples can be found in the books by Murray [22] and Edelstein-Keshet [10]. The nonlinearity f is typically a cubic or cubic-like function, and the system is considered an activator-inhibitor system in that u activates the production of w while w inhibits u. Models of this type have attracted a great deal of attention since the celebrated work of Turing [30], who proved that diffusion can have a destabilizing effect resulting in spatial pattern formation.

In recent years these models have been shown to produce a variety of interesting phenomena and have been the impetus for many new and exciting mathematical results. Nishiura [23] and Sakamoto [27] have examined the existence and stability of large amplitude spatial patterns. The formation and propagation of transition layers

has been studied by many authors (see [11] and references therein). An interesting case is the so called "breather solutions " which are solutions having oscillating layers ([24]). In terms of global dynamics, Hale [15] has demonstrated that as $D \to \infty$ the attractor of the system approaches the attractor for the so called "shadow system", which is obtained by spatially averaging (1.3). The underlying theme in each of these results is the use of perturbation techniques which exploit the extreme size of a model parameter, in particular, the cases $\epsilon \ll 1$, $\frac{1}{\delta} \ll 1$, and D large have been extensively examined. As far as we know, this thesis is the first study of the limiting equation for the case $\delta \ll 1$. Physically this corresponds to an activator-inhibitor system in which the rates of reaction and diffusion of the inhibitor greatly exceed those of the activator. The inhibition appears in the limiting equation (1.1) as nonlocal feedback.

In this work, we consider the particular model where f is the symmetric cubic polynomial $f(u) = u - u^3$, and $\gamma \geq 0$. Our goal is to gain a geometric or qualitative understanding of the global behavior of solutions to (1.1). This equation is a nonlocally perturbed version of the standard Chafee-Infante problem

$$u_t = \epsilon^2 u_{xx} + f(u), \quad u_x(0,t) = u_x(1,t) = 0, \tag{1.4}$$

for which a great deal is known (see [14] and [16]). As such, we expect the dynamics of (1.1) to inherit many of the properties of the dynamics for (1.4) when γ is sufficiently small, and we will verify this is so. However, when $\gamma = \mathcal{O}(1)$ we will see the dynamics differ considerably. In this case, the analysis is significantly complicated by the nonlocal perturbation. Classical results based on maximum principles and comparison arguments ([28]) do not apply and rigorous mathematical results are difficult to obtain. Thus, we must rely on approximation techniques and numerical simulations to gain insight.

This thesis is comprised of six chapters, the first being this introduction.

In Chapter 2, we prove the existence of local solutions for (1.1) using standard

results from linear and nonlinear semigroup theory. We show (1.1) has a Lyapunov function which allows us to obtain a global existence result. We then establish the existence of a compact, connected, invariant set which attracts all solutions. This set, called a global attractor, contains much of the information regarding the large time dynamics. The necessary ingredients for the existence of a global attractor are compactness and dissipation. Since in general partial differential equations are posed on metric spaces which are not locally compact, the necessary compactness must come from the solution operator. We establish the compactness of the solution operator for (1.1) by the use of embedding theorems much like the standard Sobolev embedding results ([1]). The concept of dissipation essentially means there is a bounded set into which all solutions enter in a finite time and remain. These properties, along with the existence of a Lyapunov function, allow us to verify (1.1) falls into a special class of systems known as gradient systems. For gradient systems the attractor has a relatively simple description: it is the union of the equilibria and their unstable manifolds. Thus, a characterization of the attractor is complete when all equilibria and their unstable manifolds are found. The goal of characterizing the attractor provides the main theme for this thesis and motivates the work of the remaining chapters.

In Chapter 3,s we search for equilibria of (1.1) by examining local bifurcations from known solutions. This is accomplished using standard techniques of bifurcation theory for Fredholm operators. Due to the nonlocal perturbation, the bifurcation diagram differs significantly from that of (1.4), and the bifurcations have a dependence on both parameters, ϵ and γ. In particular, we demonstrate the existence of an interesting family of secondary bifurcations. This is accomplished by means of a projection method, known as Lyapunov-Schmidt reduction, which allows us to reduce the equation to a two-dimensional problem in the neighborhood of certain points in

parameter space. The resulting two-dimensional system is simple and can be easily analyzed. This result generalizes a previous result obtained by Keener [20].

In Chapter 4, we show the existence of a finite-dimensional manifold containing the attractor which attracts all solutions of (1.1) at an exponential rate. This manifold, known as an inertial manifold, is the equivalent of a global center manifold for an infinite-dimensional system. The restriction of (1.1) to the inertial manifold yields a finite-dimensional system which exhibits all of the large time dynamics of (1.1). Although in general we cannot actually compute the inertial manifold or the equations on the manifold, the existence of these objects tells us that the dynamics of (1.1) are essentially finite-dimensional. In the case where ϵ is large, however, we provide proof that the large time dynamics are equivalent to the dynamics of a simple one-dimensional ordinary differential equation. We also prove the existence of a finite-dimensional manifold, known as a steady inertial manifold, which contains the equilibria for (1.1) and is, in a sense, close to the attractor. The steady inertial manifold is of low dimension and can be approximated by a sequence of manifolds, known as approximate inertial manifolds (AIMs), which can be explicitly computed. These approximations provide us with low-dimensional systems of equations which allow us to extend the local bifurcation results to larger regions in parameter space and locate the unstable manifolds of equilibria.

In Chapter 5, we use the results of the preceding chapters and simulations based on standard numerical methods to obtain a qualitative picture of subsets of the attractor in a limited parameter regime. We provide evidence for a global bifurcation picture and obtain approximations of the orbits which connect the equilibria. From the numerical evidence we obtain in this chapter, we conjecture the attractor contains a set of relatively simple two-dimensional structures.

Finally in Chapter 6, we summarize our results, especially noting the apparent

differences between the dynamics for (1.1) and (1.4). We also provide directions for future investigations.

CHAPTER 2

PRELIMINARY RESULTS

Introduction

In this chapter, we gather some preliminary mathematical results for the reaction-diffusion equation with nonlocal inhibition,

$$u_t = \epsilon^2 u_{xx} + \gamma B u + f(u), \quad u_x(0,t) = u_x(1,t) = 0, \tag{2.1}$$

where $\gamma \geq 0$. This equation corresponds to the limiting equation as $\delta \to 0$, with ϵ fixed for the singularly perturbed reaction-diffusion system,

$$\frac{du}{dt} = \epsilon^2 u_{xx} + f(u) - w, \quad u_x(0,t) = u_x(1,t) = 0, \tag{2.2}$$

$$\delta \frac{dw}{dt} = D w_{xx} + \gamma u - w, \quad w_x(0,t) = w_x(1,t) = 0. \tag{2.3}$$

To see this, we note that

$$D w_{xx} + \gamma u - w = 0 \tag{2.4}$$

can be solved for w as a function of u , $w = -\gamma B u$, where B is the nonlocal operator $Bu(x) = \int_0^1 g(x,s)u(s)ds$ with the Green's function,

$$g(x,s) = \begin{cases} -\frac{\sqrt{D}cosh(\frac{x}{\sqrt{D}})cosh(\frac{s-1}{\sqrt{D}})}{sinh(\frac{1}{\sqrt{D}})}, & 0 \leq x < s \leq 1, \\ -\frac{\sqrt{D}cosh(\frac{x-1}{\sqrt{D}})cosh(\frac{s}{\sqrt{D}})}{sinh(\frac{1}{\sqrt{D}})}, & 0 \leq s < x \leq 1. \end{cases}$$

First, we introduce some standard concepts from linear functional analysis. Then we will prove the existence of solutions and a global attractor for equation (2.1).

Operator Theory and Function Spaces

In the following, we will let $(\cdot,\cdot)_0$ and $||\cdot||_0$ denote the usual inner-product and norm on the Hilbert space $L^2(0,1)$ and $||\cdot||$ the operator norm on $L^2(0,1)$. When referring to an arbitrary normed space or Hilbert space X, we will denote the norm, and inner-product by $||\cdot||_X$, and $(\cdot,\cdot)_X$, respectively. By H^k_N we denote the closure of the cosine functions $\{cos(n\pi x)\}_{n=0}^{\infty}$ in the Sobolev space $H^k(0,1)$. For $k>1$ this is simply the elements in $H^k(0,1)$ which satisfy the homogeneous Neumann boundary conditions in the classical sense (see [1]). For $\gamma>0$, let $A: D(A)\subset L^2(0,1)\rightarrow L^2(0,1)$ be defined by

$$D(A)=H^2_N, \tag{2.5}$$

$$Au=-\epsilon^2 u''-\gamma Bu, \quad \forall u\in D(A). \tag{2.6}$$

We see that equation (2.1) can be written as the abstract evolution equation

$$u_t=-Au+f(u), \quad u(0)=u_0. \tag{2.7}$$

It follows from standard results (see [7]) that the operator A is closed, densely defined, positive, and self-adjoint. The spectrum of A consists solely of eigenvalues, which can easily be seen to be

$$\sigma_n=\epsilon^2(n\pi)^2+\frac{\gamma}{D(n\pi)^2+1}, \quad n=0,1,\ldots, \tag{2.8}$$

with normalized eigenfunctions

$$\phi_0(x)=1, \quad \phi_n(x)=\sqrt{2}cos(n\pi x), \quad n=1,2,\ldots.$$

From the spectral theorem (see [9]) it follows that

$$A^{-1}u=\sum_{n=0}^{\infty}\sigma_n^{-1}(u,\phi_n)_0\phi_n(x). \tag{2.9}$$

Thus, A^{-1} is the uniform limit of finite-dimensional operators and hence is compact. Now for any $\beta \in \mathbb{R}$ we define A^β by

$$D(A^\beta) = \left\{ u \in L^2(0,1) : \sum_{n=0}^{\infty} \sigma_n^{2\beta} |(u, \phi_n)_0|^2 < \infty \right\}$$

and

$$A^\beta u = \sum_{n=0}^{\infty} \sigma_n^\beta (u, \phi_n)_0 \phi_n(x).$$

Equipped with the graph norm, $||\cdot||_{2\beta} = ||A^\beta(\cdot)||_0$, $D(A^\beta)$ becomes a Banach space. We will need the following embedding result which is proven in [16].

Lemma 2.1 *The following embeddings hold:*

$$D(A^\alpha) \subset D(A^\beta), \quad when, \quad 0 \leq \beta \leq \alpha. \tag{2.10}$$

$$D(A^\alpha) \subset H^1(0,1), \quad when, \quad \frac{1}{2} < \alpha. \tag{2.11}$$

$$D(A^\alpha) \subset C[0,1], \quad when \quad \frac{1}{2} < 2\alpha. \tag{2.12}$$

Moreover, the embedding (2.10) is compact when the inequality is strict.

The spaces $(D(A), ||\cdot||_2)$, $\left(D(A^{1/2}), ||\cdot||_1\right)$ and $(L^2(0,1), ||\cdot||_0)$ provide us a convenient setting to analyze the nonlocal reaction-diffusion equation. The following lemma gives Poincaré type inequalities for these spaces. Note the stated form of the eigenvalues of A in equation (2.8) does not guarantee the smallest positive or principle eigenvalue of A is σ_0. In the following, σ_p will denote the principle eigenvalue.

Lemma 2.2 *The following inequalities hold:*

$$\sqrt{\sigma_p}||u||_0 \leq ||u||_1, \quad \forall u \in D(A^{1/2}). \tag{2.13}$$

$$\sqrt{\sigma_p}||u||_1 \leq ||u||_2, \quad \forall u \in D(A). \tag{2.14}$$

Proof: Let $u \in D(A^{1/2})$, then $u = \sum_{n=0}^{\infty} u_n \phi_n$ and $A^{1/2}u = \sum_{n=0}^{\infty} \sqrt{\sigma_n} u_n \phi_n$, hence

$$||u||_1^2 = \sum_{n=0}^{\infty} \sigma_n u_n^2 \geq \sigma_p \sum_{n=0}^{\infty} u_n^2 = \sigma_p ||u||_0^2,$$

and the first inequality is proved. To establish (2.14), let $u \in D(A)$ and $Au = \sum_{n=0}^{\infty} a_n \phi_n$. Then $u = \sum_{n=0}^{\infty} \frac{a_n}{\sigma_n} \phi_n$ and

$$||u||_1^2 = \sum_{n=0}^{\infty} \frac{a_n}{\sigma_n}^2 \leq \frac{1}{\sigma_p} \sum_{n=0}^{\infty} a_n^2 \leq \frac{1}{\sigma_p} ||u||_2^2.$$

□

Definition 2.3 *An* **analytic semigroup** *on a Banach space X is a family of continuous linear operators on X, $\{T(t)\}_{t \geq 0}$, satisfying:*

1. *$T(0) = I$, $T(t)T(s) = T(t+s)$ for $t, s \geq 0$.*
2. *$T(t)u \to u$ as $t \to 0^+$ for each $u \in X$.*
3. *The map $t \to T(t)u$ is real analytic on $0 < t < \infty$ for each $u \in X$.*

The **infinitesimal generator** *of a semigroup $T(t)$ is the linear operator L defined by*

$$Lu = \lim_{t \to 0^+} \frac{1}{t}(T(t)u - u),$$

with domain $D(L)$ consisting of all $u \in X$ for which this limit exists. It is standard notation to write $T(t) = e^{Lt}$.

The following theorem, which is proven in [25], provides sufficient conditions for L to be the generator of an analytic semigroup.

Theorem 2.4 *Let L be a closed, densely defined, linear operator on a Banach space X. If there exist constants $\theta \in (0, \frac{\pi}{2})$, and $M > 0$ such that*

$$\Sigma = \left\{ \lambda \in \mathbb{C} : |arg\lambda| \leq \frac{\pi}{2} + \theta \right\} \cup \{0\} \subset \rho(L), \tag{2.15}$$

were $\rho(L)$ is the resolvent set of L, and

$$||(\lambda I - L)^{-1}|| \leq \frac{M}{|\lambda|}, \quad \forall \lambda \in \Sigma, \quad \lambda \neq 0. \tag{2.16}$$

Then L is the infinitesimal generator of an analytic semigroup on X.

An operator which satisfies the hypotheses of the theorem is called a sectorial operator. To see that $-A$ generates an analytic semigroup on $L^2(0,1)$, note that the spectrum of $-A$ consists of real, negative eigenvalues. Thus, (2.15) holds for any $\theta \in (0, \frac{\pi}{2})$. To verify (2.16), consider the spectral representation of the resolvent operator,

$$(\lambda I + A)^{-1} u = \sum_{n=0}^{\infty} \frac{(u, \phi_n)_0}{\lambda + \sigma_n} \phi_n(x).$$

From this we see

$$||(\lambda I + A)^{-1} u||_0 \leq \sum_{n=0}^{\infty} \frac{|(u, \phi_n)_0|}{|\lambda + \sigma_n|}, \tag{2.17}$$

but for all $\theta \in (0, \frac{\pi}{2})$ and $\lambda \neq 0$ such that $|arg\lambda| < \frac{\pi}{2} + \theta$,

$$\frac{1}{|\lambda + \sigma_n|} \leq \frac{csc(\frac{\pi}{2} + \theta)}{|\lambda|}, \quad \forall n.$$

Therefore,

$$||(\lambda I + A)^{-1}|| \leq \frac{csc(\frac{\pi}{2} + \theta)}{|\lambda|}, \quad \lambda \in \Sigma. \tag{2.18}$$

The semigroup e^{-At} has a simple representation

$$e^{-At} u = \sum_{n=0}^{\infty} e^{-\sigma_n t} (u, \phi_n)_0 \phi_n(x)$$

from which we obtain the uniform decay estimate, $||e^{-At}|| \leq e^{-\sigma_p t}$, for all $t \geq 0$.

We will need the following standard result, which is proven in [25].

Lemma 2.5 *Let $-A$ be the infinitesimal generator of an analytic semigroup e^{-At} on a Hilbert space H with $0 \in \rho(A)$. Also, assume $||e^{-At}|| \leq Me^{-\omega t}$ for some $M > 0$ and $\omega \in \mathbb{R}$, where $||\cdot||$ is the operator norm on H. Then:*

1. *$e^{-At} : H \mapsto D(A^\alpha)$ for every $t > 0$ and $\alpha \geq 0$.*
2. *For every $u \in D(A^\alpha)$, $A^\alpha e^{-At} u = e^{-At} A^\alpha u$.*
3. *For every $t > 0$ the operator $A^\alpha e^{-At}$ is bounded and $||A^\alpha e^{-At}|| \leq M_\alpha t^{-\alpha} e^{-\omega t}$, for some $M_\alpha > 0$.*

Existence of Solutions and the Global Attractor

To discuss the existence of solutions and a global attractor for equation (2.7) we need the notion of a nonlinear semigroup, which acts as the solution operator for (2.7). The results here essentially follow the presentation in [14].

Definition 2.6 *Let X be a complete metric space. A family of mappings $S(t) : X \to X$, $t \geq 0$, is said to be a C^r-***semigroup***, $r \geq 0$, provided :*

1. $S(0) = I$.
2. $S(t+s) = S(t)S(s), \quad s, t \geq 0$.
3. *$S(t)u$ is continuous in t and u together with Frechét derivatives in u through order r for $(t, u) \in [0, \infty) \times X$.*

For completeness we recall the definition of the Frechét derivative.

Definition 2.7 *Let X and Y be Banach spaces. The* **Frechét derivative** *of an operator $T : X \to Y$ at a point $x \in X$ is a continuous linear operator $L : X \to Y$ such that*

$$T(x+h) - T(x) = Lh + R(x,h), \tag{2.19}$$

where $\frac{||R(x,h)||_Y}{||h||_X} \to 0$ as $||h||_X \to 0$.

To fix our notation, throughout this work we will denote the Frechét derivative with respect to a variable x of a mapping T at point x_1 by $D_x T(x_1)$.

In the following definitions, we assume $\{S(t), t \geq 0\}$ is a semigroup on a Banach space X.

Definition 2.8 *The* **ω-limit set** *of a point $u_0 \in X$ and a subset $B \subset X$ are defined as*

$$\omega(u_0) = \bigcap_{s \geq 0} \overline{\bigcup_{t \geq s} S(t)u_0},$$

$$\omega(B) = \bigcap_{s \geq 0} \overline{\bigcup_{t \geq s} S(t)B},$$

where $\overline{\cdot}$ *denotes the closure of the set.*

Definition 2.9 *A subset* $B \subset X$ *is said to be* **invariant** *if*

$$S(t)B = B, \quad \forall t \geq 0.$$

Example 2.10 *A point* $u \in X$ *is an equilibrium point for a semigroup* $S(t)$ *on* X *if and only if* $S(t)u = u$ *for all* $t \geq 0$. *Thus we see equilibria are invariant sets.*

Other examples of invariant sets include the stable and unstable manifolds of equilibria, whose definition we now provide.

Definition 2.11 *The* **stable manifold**, $W^s(u)$, *and the* **unstable manifold**, $W^u(u)$, *of an equilibrium point* u *for* $S(t)$ *are defined as*

$$W^s(u) = \{x \in X : S(t)x \ \ is \ \ defined \ \ \forall t \geq 0, \ \ and \ \ S(t)x \to u \ \ as \ \ t \to \infty\},$$

$$W^u(u) = \{x \in X : S(t)x \ \ is \ \ defined \ \ \forall t \leq 0, \ \ and \ \ S(t)x \to u \ \ as \ \ t \to -\infty\}.$$

Definition 2.12 *A set* $\mathcal{B} \subset X$ *is said to* **attract** *a set* $U \subset X$ *under* $S(t)$ *if* $dist(S(t)U, \mathcal{B}) \to 0$ *as* $t \to \infty$.

Definition 2.13 *An invariant set* $\mathcal{A}$ *is said to be the* **global attractor** *for a semigroup* $S(t)$ *if* $\mathcal{A}$ *is a maximal, compact, invariant set which attracts each bounded set* $U \subset X$.

If a system has a global attractor, then the ω-limit set of each bounded set is contained in the global attractor. Therefore, much of the dynamic behavior of the system is determined by the restriction of the semigroup to the attractor. Although transient behavior may be important, understanding the dynamics on the attractor is a natural place to begin exploring the global dynamics of the evolution equation.

The notion of dissipation is an important property of a dynamical system which roughly corresponds to the lack of a conservation law for the system. The particular form of dissipation we will use, point dissipation, is defined as follows:

Definition 2.14 *A semigroup $S(t)$ is said to be* **point dissipative** *if there is a bounded set $\mathcal{B} \subset X$ that attracts each point of X under $S(t)$.*

For finite-dimensional systems, point dissipation is sufficient to guarantee the existence of a global attractor. This is due to the fact that finite-dimensional Banach spaces are locally compact. Since infinite-dimensional Banach spaces are not locally compact, we need a degree of compactness from the semigroup itself to obtain the desired results. Many semigroups generated by evolution equations possess a "smoothing" property which is equivalent to the notion of compactness of the operator.

Definition 2.15 *The semigroup $S(t)$ is said to be* **eventually compact** *if for each bounded set B, there exists a T such that $\bigcup_{t \geq T} S(t)B$ is relatively compact in X.*

The following theorem, whose proof can be found in [14], provides sufficient conditions for the existence of a global attractor for point dissipative systems.

Theorem 2.16 *Let $S(t)$ be an eventually compact, point dissipative C^r-semigroup on a complete metric space X such that for each bounded set $U \in X$, the set*

$$\{S(t)u : t \geq 0, u \in U\}$$

is bounded. Then there exists a global attractor $\mathcal{A}$. If X is a Banach space, then $\mathcal{A}$ is connected. If, in addition, $S(t)$ is one-to-one on $\mathcal{A}$ then $S(t)|_{\mathcal{A}}$ is a C^r-group.

Before proceeding to verify the hypotheses of the above theorem, we need to show the existence of a semigroup for equation (2.7). Let $f^e : D(A) \to L^2(0,1)$ be

defined by $f^e(u)(x) = f(u(x))$. By (2.12), given $r_1 > 0$ there exists an $r_2 > 0$ so that for $u, v \in D(A^{1/2})$ with $||u||_1, ||v||_1 \leq r_1$ we have $|u|, |v| \leq r_2$ for all $x \in [0,1]$. Now

$$||f(u) - f(v)||_0^2 = \int_0^1 [f(u(x)) - f(v(x))]^2 \, dx, \tag{2.20}$$

$$= \int_0^1 \left[\int_{v(x)}^{u(x)} f'(s) ds \right]^2 dx. \tag{2.21}$$

But there exists a constant c which depends on r_2 such that

$$\left| \int_{v(x)}^{u(x)} f'(s) ds \right| \leq c|u(x) - v(x)|, \quad \forall x \in [0,1]$$

and therefore by Lemma 2.2,

$$||f^e(u) - f^e(v)||_0^2 \leq c^2 \int_0^1 [u(x) - v(x)]^2 \, dx \leq \frac{c^2}{\sigma_p} ||u - v||_1^2.$$

Thus, f^e is locally Lipschitz continuous. In the following, we will not distinguish between f as a function on the real numbers and f^e as a mapping between function spaces, rather we will denote both by f. The equation is now locally well posed in $D(A^{1/2})$.

Lemma 2.17 *For initial data, $u_0 \in D(A^{1/2})$, the evolution equation (2.7) has a unique local solution in $C((0,T), D(A)) \cap C([0,T), D(A^{1/2}))$. Moreover, either $T = \infty$ or $||u(t)||_1 \to \infty$ as $t \to T$. Also, the mapping $t \mapsto \frac{du(t)}{dt} \in D(A^{1/2})$ is locally Hölder continuous on $(0,T)$.*

Proof: The proof follows from Theorems 3.3.3, 3.3.4, and 3.5.2 of [16]. □

To show the solution is globally defined, it suffices to show that solutions remain bounded in $D(A^{1/2})$ as $t \to T$. To see this, consider the function $V : D(A^{1/2}) \to \mathbb{R}$ defined by

$$V(u) = \frac{1}{2}||u||_1^2 + \int_0^1 \left(\frac{u^4}{4} - \frac{u^2}{2} \right) dx.$$

If $u(t)$ is a local solution on $[0,T)$, then

$$\frac{dV(u)}{dt} = \left(A^{1/2}u, A^{1/2}\frac{du}{dt}\right)_0 - \left(f(u), \frac{du}{dt}\right)_0, \tag{2.22}$$

$$= \left(Au, \frac{du}{dt}\right)_0 - \left(f(u), \frac{du}{dt}\right)_0, \tag{2.23}$$

$$= \left(Au - f(u), \frac{du}{dt}\right)_0, \tag{2.24}$$

$$= -||\frac{du}{dt}||_0^2 \leq 0. \tag{2.25}$$

Thus, V is a nonincreasing function of t along local solutions. Now for each $k > 0$ there exists a C_k so that $\frac{s^2}{2} - \frac{s^4}{4} < ks^2 + C_k, \quad \forall s \in \mathbb{R}$. Therefore,

$$V(u) \geq \frac{1}{2}||u||_1^2 - k||u||_0^2 - C_k, \tag{2.26}$$

and by Lemma 2.2,

$$V(u) + C_k \geq \frac{1}{2}||u||_1^2 - \frac{k}{\sigma_p}||u||_1^2. \tag{2.27}$$

Choosing $k < \frac{\sigma_p}{2}$ we have

$$V(u(0)) + C_k \geq V(u(t)) + C_k \geq (\frac{1}{2} - \frac{k}{\sigma_p})||u||_1^2 \geq 0, \quad t \in [0,T), \tag{2.28}$$

and the solution is uniformly bounded on $[0,T)$. Therefore, by Lemma 2.17, solutions are defined for all time and the equation generates a nonlinear semigroup $\mathcal{S}(t)$ on $D(A^{1/2})$.

The function V defined above is known as a Lyapunov function, and for completeness we provide the following definition.

Definition 2.18 *A* **Lyapunov function** *for a semigroup $S(t)$ on a metric space X is a continuous real valued function $V : X \to \mathbb{R}$ such that*

$$\frac{dV(u_0)}{dt} = \limsup_{t \to 0^+} \frac{1}{t}\{V(S(t)u_0) - V(u_0)\} \leq 0, \quad \forall u_0 \in X.$$

To show the existence of a global attractor, it remains to verify that $\mathcal{S}(t)$ is compact and point dissipative. To verify the compactness of $\mathcal{S}(t)$, it suffices to show that orbits remain bounded in $D(A^\beta)$, for $\frac{1}{2} < \beta < 1$. The relative compactness of the orbits follows from the compactness of the embedding $D(A^\beta) \subset D(A^{1/2})$. To see that solutions of (2.7) are bounded in $D(A^\beta)$, note that if $u(t)$ is a solution with $u(0) = u_0$, then

$$A^\beta u(t) = A^\beta e^{-At}u_0 + \int_0^t A^\beta e^{-A(t-s)} f(u(s))ds, \tag{2.29}$$

$$= A^{\beta-1/2}e^{-At}A^{1/2}u_0 + \int_0^t A^\beta e^{-A(t-s)} f(u(s))ds, \tag{2.30}$$

and by Lemma 2.5,

$$||A^\beta u(t)||_0 \leq M_{\beta-1/2}t^{\beta-1/2}e^{-\sigma_p t}||u_0||_1 + M_\beta \int_0^t (t-s)^{-\beta}e^{-\sigma_p(t-s)}||f(u(s))||_0 ds.$$

Since $u(t)$ is bounded in $D(A^{1/2})$ and $f : D(A^{1/2}) \to L^2(0,1)$ is locally Lipschitz, there is a constant C depending on u_0 such that $||f(u(t))||_0 \leq C$ for all $t \geq 0$. Therefore,

$$||A^\beta u(t)||_0 \leq M_{\beta-1/2}t^{\beta-1/2}e^{-\sigma_p t}||u_0||_1 + M_\beta C \int_0^t (t-s)^{-\beta}e^{-\sigma_p(t-s)} ds,$$

which is bounded for all $t > 0$. Hence, the nonlinear semigroup is compact.

To verify the semigroup is point dissipative, we need the following result which can be found in [16].

Lemma 2.19 *Let $S(t)$ be a semigroup on a Banach space X. Suppose $u_0 \in X$ and $\{S(t)u_0, t \geq 0\}$ lies in a compact set in X, then $\omega(u_0)$ is nonempty, compact, connected, invariant and dist$(S(t)u_0, \omega(u_0)) \to 0$ as $t \to +\infty$.*

Now define $E = \left\{u \in D(A^{1/2}) : \frac{dV(S(t)u)}{dt} = 0\right\}$ and let $\mathcal{M}$ be the maximal invariant set of E. The set $\mathcal{M}$ will be our candidate for a bounded attracting set. To see that $\mathcal{M}$ is bounded in $D(A^{1/2})$, first note that by equation (2.25), $u \in E$ if and only if u is an equilibrium solution. Therefore,

$$||u||_1^2 = (A^{1/2}u, A^{1/2}u)_0 = (u, Au)_0 = (u, f(u))_0 = \int_0^1 \left(u^2 - u^4\right) dx.$$

But $s^2 - s^4 \leq \frac{1}{4}$, for all $s \in \mathbb{R}$ and thus $||u||_1^2 \leq \frac{1}{4}$ for all $u \in E$. By the estimate of equation (2.27) with $k < \frac{\sigma_p}{2}$, we see that V is bounded below. Hence, $V(\mathcal{S}(t)u_0)$ is a continuous nonincreasing function that is bounded below and therefore $l(u_0) \equiv \lim_{t\to\infty} V(\mathcal{S}(t)u_0)$ exists. If $y \in \omega(u_0)$, then $V(y) = l(u_0)$ and so $V(\mathcal{S}(t)y) = l(u_0)$ for all $t \in \mathbb{R}$. Thus, $y \in E$ and $\omega(u_0) \in \mathcal{M}$. It follows that $\mathcal{M}$ is globally attracting and the semigroup is point dissipative. We have proven the following theorem:

Theorem 2.20 *The nonlocal reaction-diffusion equation has a global attractor $\mathcal{A}$ which is connected in $D(A^{1/2})$.*

The semigroup for the evolution equation falls into a special class of systems, known as gradient systems, for which the flow on the attractor can be described with some detail.

Definition 2.21 *A C^r-semigroup $S(t)$ on a Banach space X is said to be a gradient system if:*

1. *Each bounded positive orbit is relatively compact.*
2. *There is a Lyapunov function $V : X \to \mathbb{R}$ for $S(t)$ such that,*
   - *(a) V is bounded below.*
   - *(b) $V(u) \to \infty$ as $||u||_X \to \infty$.*
   - *(c) $V(S(t)u)$ is nonincreasing in t for each $u \in X$.*
   - *(d) If u is such that $V(S(t)u) = V(u)$ for all $t \in \mathbb{R}$ then u is an equilibrium.*

Since the semigroup $\mathcal{S}(t)$ generated by (2.7) is a gradient system, it is known (see [14]) the attractor consists of the unstable manifolds of the set E, that is

$$\mathcal{A} = \left\{u \in D(A^{1/2}) : \mathcal{S}(-t)u \quad exists \quad for \quad t \geq 0 \quad and \quad \mathcal{S}(-t)u \to E \quad as \quad t \to \infty\right\}.$$

Definition 2.22 *An equilibrium u_0 for a semigroup $S(t)$ is said to be* **hyperbolic** *if the spectrum of $D_u S(t)u_0$ does not intersect the unit circle centered at zero in $\mathbb{C}$.*

For $\mathcal{S}(t)$ this definition is equivalent to the condition that zero is not in the spectrum of the linear operator $\mathcal{L} : D(A) \to L^2(0,1)$ defined by

$$\mathcal{L}\phi \equiv -A\phi + f'(u_0)\phi, \quad \phi \in D(A). \tag{2.31}$$

If E consists of hyperbolic equilibria then it is necessarily finite and

$$\mathcal{A} = \bigcup \{W^u(\phi) : \phi \in E\}.$$

Away from bifurcations all equilibria of equation (2.7) are hyperbolic, hence a characterization of the attractor is complete when all of the equilibria and unstable manifolds are found.

CHAPTER 3

BIFURCATION RESULTS

Introduction

Due to the gradient structure of the equation (2.1), we know that when the equilibria are hyperbolic the attractor consists of the equilibria and their unstable manifolds. Therefore, the characterization of the attractor is complete when the equilibria and connecting orbits are found. Our equation is a nonlocal perturbation of the standard Chafee-Infante problem

$$u_t = \epsilon^2 u_{xx} + f(u), \quad u_x(0,t) = u_x(1,t) = 0, \tag{3.1}$$

for which a great deal is known. In fact, for any value of ϵ a complete description of the attractor can be given and a summary of results can be found in [14] and [16]. The steady state equation is a planar system which can easily be analyzed and all equilibria located. Spatially heterogeneous solutions occur as bifurcations from the zero solution at $\epsilon = \frac{1}{n\pi}$, for $n = 1, 2, \ldots$. For each n, the bifurcation is a pitchfork which yields a pair of solutions which are $n\pi$-periodic and continue to large amplitude patterns having n internal transition layers as $\epsilon \to 0$. These solutions are unstable with the dimension of the unstable manifolds being equal to the number of internal transition layers. It has been shown that for two equilibria u^+, u^- a heteroclinic connection between them exists if and only if $dim\,(W^u(u^-)) \neq dim\,(W^u(u^+))$ and the flow proceeds in the direction as to decrease the number of transition layers. Moreover, if u^- and u^+ are hyperbolic equilibria and $dim\,(W^u(u^-)) > dim\,(W^u(u^+))$,

then $W^u(u^-)$ and $W^s(u^+)$ intersect transversally. For small values of γ we should expect the structure of the attractor for (2.1) to be similar to that of (3.1). To see this, note that for ϵ fixed

$$\mathcal{F}(u, \epsilon, \gamma) = \epsilon^2 u'' + f(u) + \gamma B u \tag{3.2}$$

is a C^2 map from $D(A) \times \mathbb{R}$ into $L^2(0,1)$. It is in fact analytic. If u_0 is a hyperbolic equilibria of (3.1) then $\mathcal{F}(u_0, \epsilon, 0) = 0$, $D_u\mathcal{F}(u, \epsilon, \gamma)$ is continuous in u and γ in a neighborhood of $(u_0, 0)$ and $D_u\mathcal{F}(u_0, \epsilon, 0)$ is nonsingular. Therefore, by the implicit function theorem (see [31]) there is a solution curve $(u(\gamma), \gamma)$ passing through $(u_0, 0)$ for γ small. This curve is analytic in γ and can be written as $u(x, \gamma) = u_0(x) + \gamma u_1(x, \gamma)$. Thus, the equilibria perturb smoothly. Now since $\mathcal{F}$ is analytic in γ, so is the nonlinear semigroup $\mathcal{S}(t)$ (see [16]). Assume $u_0^-(x)$ and $u_0^+(x)$ are hyperbolic equilibria of (3.1) and a heteroclinic connection exists between them. Let $u^-(x, \gamma) = u_0^-(x) + \gamma u_1^-(x, \gamma)$ and $u(x, \gamma)^+ = u_0^+(x) + \gamma u_1^+(x, \gamma)$ be solutions of (3.2), through $(u_0^-, 0)$ and $(u_0^+, 0)$, respectively. Assume also that for all γ sufficiently small these equilibria remain hyperbolic. Then the heteroclinic connection, being the transverse intersection of the stable and unstable manifolds, perturbs continuously for all γ sufficiently small. That is, the connection perturbs to a connection between the equilibria of (2.1).

Unfortunately, when γ is large the nonlocal perturbation γB complicates matters significantly. No longer can we locate the equilibria by phase plane analysis. The results concerning heteroclinic connections for the Chafee-Infante problem rely on the strong maximum principle which does not hold for the operator A when $\gamma > 0$. The goal of this work is to begin a program of characterizing the global attractor for the case where γ is not necessarily small. In this chapter, we perform local bifurcation analysis in order to locate equilibria. As we will see, the global bifurcation picture for (2.1) promises to be much more interesting than that of the Chafee-Infante problem

in that it includes secondary bifurcations.

Bifurcations from Simple Eigenvalues

The main bifurcation result we will use is a standard theorem of Crandall and Rabinowitz [6] concerning bifurcations from a simple eigenvalue of Fredholm operators.

Definition 3.1 *Let X and Y be Banach spaces. A bounded linear operator $L : X \to Y$ is called* **Fredholm** *if the following two conditions hold:*

1. *The null space of L, $N(L)$, is a finite-dimensional subspace of X.*
2. *The range of L, $R(L)$, is closed and has finite codimension.*

The **Fredholm index** *of L is the integer*

$$ind(L) = dim\,(N(L)) - codim\,(R(L))\,. \tag{3.3}$$

We will need the following result, whose proof can be found in [31]. The first two statements of the theorem are known as the Fredholm alternative, which concerns the existence of solutions of the equation

$$Lx = y \tag{3.4}$$

for Fredholm operators. Although the result can be stated for operators on Banach spaces, we will use a version for operators on Hilbert spaces X and Y.

Theorem 3.2 *For a Fredholm operator $L : X \to Y$ the following are true:*

1. *If $ind(L) = 0$ and $N(L) = 0$ then (3.4) has exactly one solution for every $y \in Y$ and $L^{-1} : Y \to X$ is a bounded linear operator.*

2. *For $y \in Y$, (3.4) has a solution if and only if $(y^*, y)_Y = 0$ for all $y^* \in N(L^*)$, where $L^* : Y \to X$ is the adjoint of L.*

3. *The adjoint operator L^* is also Fredholm and*

$$dim(N(L^*)) = codim(R(L)), \tag{3.5}$$

$$codim(R(L^*)) = dim(N(L)), \tag{3.6}$$

$$ind(L^*) = -ind(L). \tag{3.7}$$

4. *If $K : X \to Y$ is a linear operator that is compact or bounded, then $L + K$ is Fredholm and*

$$ind(L + K) = ind(L). \tag{3.8}$$

Example 3.3 *It is easy to verify that the second derivative operator $\epsilon^2 \frac{d^2}{dx^2} : D(A) \to L^2(0,1)$ is a Fredholm operator with zero index. By the previous theorem, for any $a \in C[0,1]$ and compact operator $K : D(A) \to L^2(0,1)$, the operator $L : D(A) \to L^2(0,1)$ defined by*

$$Lu = \epsilon^2 u'' + a(x)u + Ku, \quad u \in D(A), \tag{3.9}$$

is a zero index Fredholm operator.

The following theorem of Crandall and Rabinowitz, provides sufficient conditions for bifurcations from known solutions. The proof of this result can be found in [6] and [31].

Theorem 3.4 (Crandall and Rabinowitz) *Let X and Y be Hilbert spaces, U an open neighborhood of $(0,0)$ in $X \times \mathbb{R}$ and $G : U \subset X \times \mathbb{R} \to Y$ a function which is C^2 at $(0,0)$. Assume also that $G(0,\alpha) = 0$ for all $\alpha \in (-\delta, \delta)$ for some $\delta > 0$, and $L \equiv D_x G(0,0)$ is a Fredholm operator with index zero. If*

$$dim(N(L)) = 1, \quad N(L) = span\{x_0\}, \quad and \tag{3.10}$$

$$L_1 x_0 \equiv D_\alpha D_x G(0,0)x_0 \notin R(L), \tag{3.11}$$

then $(0,0)$ *is a bifurcation point and there exists a curve* $s \mapsto (x(s), \alpha(s))$ *through* $(0,0)$ *for* $|s|$ *sufficiently small so that*

$$G(x(s), \alpha(s)) = 0. \tag{3.12}$$

In a sufficiently small neighborhood of $(0,0)$ *every solution is either on the curve or of the form* $(0,\alpha)$. *On the curve,* x *is given by* $x(s) = sx_0 + sy(s)$, *where* $(y(s), x_0)_X = 0$. *Moreover, if* G *is analytic at* $(0,0)$ *then the curve can be written as an absolutely convergent power series in* s,

$$x(s) = sx_0 + \sum_{k=2}^{\infty} s^k x_k, \quad (x_0, x_k)_X = 0, \quad k \neq 0, \tag{3.13}$$

$$\alpha(s) = \sum_{k=0}^{\infty} s^k \alpha_k. \tag{3.14}$$

Condition (3.10) means zero is a simple eigenvalue of L. The condition (3.11), known as the transversality condition, says the line $L_1(N(L))$ and the hyperplane $R(L)$ intersect transversely at the origin, meaning together they span the range space Y. This condition guarantees that at the bifurcation point the critical eigenvalue passes through zero with nonzero speed.

We will use this theorem to find bifurcations from the constant solutions of the steady state equation

$$\mathcal{F}(u, \epsilon, \gamma) = \epsilon^2 u'' + f(u) + \gamma B u = 0, u \in D(A). \tag{3.15}$$

The restriction of (3.15) to the subspace of constant functions is simply the polynomial equation

$$f(u) - \gamma u = 0. \tag{3.16}$$

Real solutions of (3.16) are the only constant solutions of (3.15). When $\gamma > 1$, the only real solution of (3.16) is the zero solution and as γ passes through 1 the zero solution under goes a pitchfork bifurcation which yields a pair of solutions , $m_0^{\pm} = \pm\sqrt{1-\gamma}$.

We will look for bifurcations from the constant solutions by fixing one parameter while allowing the other to play the role of the bifurcation parameter. First, consider bifurcations as ϵ is varied. Assume γ is fixed and u is a solution of (3.16). It follows that u is a solution for all ϵ. Now suppose at ϵ_0 , zero is a simple eigenvalue of the linear operator $\mathcal{L} : D(A) \to L^2(0,1)$ given by

$$\mathcal{L}\phi \equiv \epsilon_0^2\phi'' + f'(u)\phi + \gamma B\phi \tag{3.17}$$

and let $N(\mathcal{L}) = span\{u_0\}$. From Example 3.3, we see that $\mathcal{L}$ is a zero index Fredholm operator. Now define $G : D(A) \times \mathbb{R} \to L^2(0,1)$ by

$$G(v,\alpha) = (\epsilon_0 + \alpha)^2 v'' + f(u+v) + \gamma B(u+v). \tag{3.18}$$

Then G is analytic in both variables and

$$D_v G(0,0)\phi = \epsilon_0^2\phi'' + f'(u)\phi + \gamma B\phi = \mathcal{L}\phi, \tag{3.19}$$

$$\mathcal{L}_1\phi \equiv D_\alpha D_v G(0,0)\phi = 2\epsilon_0\phi''. \tag{3.20}$$

The eigenfunctions of $\mathcal{L}$ are $\{cos(n\pi x)\}_{n=0}^{\infty}$, and therefore u_0 is a nonzero scalar multiple of $cos(n\pi x)$ for some n. From this we see that

$$\mathcal{L}_1 u_0 = -2\epsilon_0(n\pi)^2 u_0 \in N(\mathcal{L}), \tag{3.21}$$

and the transversality condition holds provided $n \neq 0$. When $n = 0$, u_0 is a constant function and $\mathcal{L}u_0 = 0$ implies

$$0 = \mathcal{L}u_0 = f'(u)u_0 - \gamma u_0, \tag{3.22}$$

from which we have $f'(u) = \gamma$ and $u = \pm\sqrt{\frac{1-\gamma}{3}}$. However, $u = \pm\sqrt{\frac{1-\gamma}{3}}$ is a solution of (3.2) if and only if $\gamma = 1$ and $u = 0$. In this case, the constant functions are in $N(\mathcal{L})$ for all values of ϵ and Theorem 3.4 does not apply. This case will be considered later when we examine secondary bifurcations. Thus, we see under the assumption $\gamma \neq 1$,

a sufficient condition for a bifurcation to occur at ϵ_0 is that $\mathcal{L}$ has a zero eigenvalue which is simple.

To consider the case where γ plays the role of the bifurcation parameter, let $u(\gamma)$ be a solution curve of (3.15) for γ in some open interval $S = (a, b)$, and ϵ fixed. Suppose at $\gamma_0 \in S$ zero is a simple eigenvalue of $\mathcal{L} : D(A) \to L^2(0,1)$ defined by

$$\mathcal{L}\phi \equiv \epsilon^2\phi'' + f'(u(\gamma_0))\phi + \gamma_0 B\phi. \tag{3.23}$$

Define $G : D(A) \times S \to L^2(0,1)$ by

$$G(v, \alpha) = \epsilon^2 v'' + f(u(\gamma_0 + \alpha) + v) + (\gamma_0 + \alpha)B(u(\gamma_0 + \alpha) + v). \tag{3.24}$$

Then

$$D_v G(0,0) = \mathcal{L}, \tag{3.25}$$

and $\mathcal{L}_1$ is given by

$$\mathcal{L}_1\phi \equiv f''(u(\gamma_0))\frac{\partial u(\gamma_0)}{\partial \gamma}\phi + \gamma_0 B\phi = \begin{cases} 3\phi + \gamma_0 B\phi, & u(\gamma_0) \neq 0, \\ \gamma_0 B\phi, & u(\gamma_0) = 0. \end{cases} \tag{3.26}$$

As in the previous case we see $\mathcal{L}_1 N(\mathcal{L}) \subset N(\mathcal{L})$ and thus the transversality condition holds.

Bifurcations from the Zero Solution

The natural place to begin looking for solutions is to search for those which bifurcate from the zero solution. We have already examined the case of the constant solutions, $m_0^{\pm} = \pm\sqrt{1-\gamma}$, bifurcating from zero. We will now consider bifurcations which result in nonconstant solutions. We shall soon see, as in the case for the Chafee-Infante problem, modal bifurcations from the zero solution occur in a predictable way as ϵ is decreased with γ fixed. However, we must also consider the dependence on the parameter γ.

Modal Bifurcations from the Zero Solution

Let

$$\mathcal{E} = \{(\gamma, \epsilon) \in \mathbb{R}^2 : \gamma \geq 0, \epsilon \geq 0\} \tag{3.27}$$

denote the parameter space for our bifurcation analysis. Linearizing (2.1) about the zero solution we obtain the eigenvalue problem

$$\mathcal{L}\phi \equiv \epsilon^2\phi'' + \phi + \gamma B\phi = \mu\phi, \quad \phi'(0) = \phi'(1) = 0, \tag{3.28}$$

which has solutions

$$\mu_n = 1 - \epsilon^2(n\pi)^2 - \frac{\gamma}{D(n\pi)^2 + 1}, \tag{3.29}$$

$$\phi_n = cos(n\pi x), \quad n = 0, 1, \ldots. \tag{3.30}$$

The equations, $\mu_n = 0$, define a family of curves $\{M_n\}_{n=0}^{\infty}$ in parameter space along which $\mathcal{L}$ has a zero eigenvalue. We will refer to these curves as the primary bifurcation curves. Specifically

$$M_n = \{(\gamma, \epsilon) \in \mathcal{E} : \gamma = (1 - (\epsilon n\pi)^2)(D(n\pi)^2 + 1)\}. \tag{3.31}$$

The curves M_0 through M_3 with $D = 1$ are plotted in Figure 1. For $m \neq n$, $M_n \cap M_m$ is nonempty and consists of a single point $C_{m,n}$ given by $C_{m,n} = (\gamma_{m,n}, \epsilon_{m,n})$ where

$$\gamma_{m,n} = \frac{(D(n\pi)^2 + 1)(D(m\pi)^2 + 1)}{D\pi^2(n^2 + m^2) + 1}, \tag{3.32}$$

$$\epsilon_{m,n} = \sqrt{\frac{D}{D(n\pi)^2 + D(m\pi)^2 + 1}}. \tag{3.33}$$

On the curve segments

$$M_n / \bigcup_{n=0}^{\infty} C_{m,n} \tag{3.34}$$

zero is a simple eigenvalue of $\mathcal{L}$ with $N(\mathcal{L}) = span\{cos(n\pi x)\}$. Theorem 3.4 holds and bifurcations occur as these curves are crossed transversally by varying one of the two parameters, ϵ or γ.

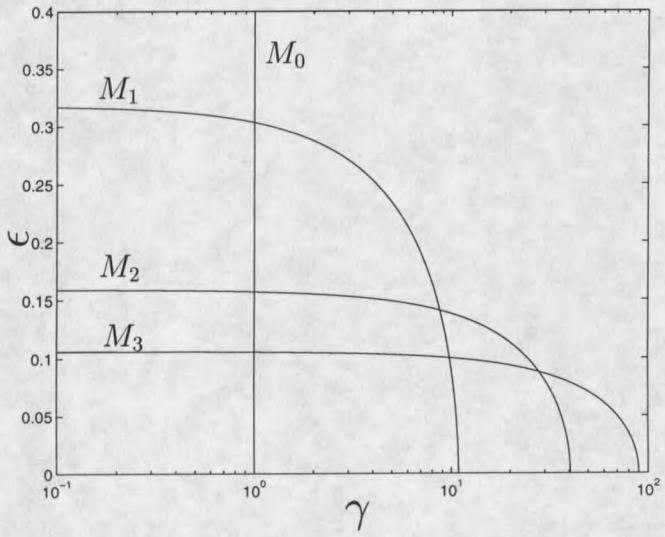


Figure 1: Primary bifurcation curves for modes 0, 1, 2 and 3.

At the intersection points, $C_{m,n}$, $N(\mathcal{L}) = span\{cos(n\pi x), cos(m\pi x)\}$ and we cannot use the Crandall-Rabinowitz theorem. As we shall see in a later section, this condition suggests the existence of secondary bifurcations.

Computation of the Local Solution Branch

From the bifurcation curves (3.31) we see that the zero solution of (3.15) can undergo a sequence of bifurcations which depends on the path taken in parameter space. To determine the local structure and stability of the bifurcating solutions, we will consider crossings of the bifurcation curves as ϵ is varied while fixing γ in such a way that we remain away from the intersection points. A similar analysis can be performed by fixing ϵ and allowing γ to vary. Consider a bifurcation of the n^{th} mode which occurs at $(\gamma, \epsilon_0) \in M_n / \bigcup_{n=0}^{\infty} C_{m,n}$. We will obtain the local solutions branch as a power series in a variable s by assuming $u = \sum_{k\geq 1} s^k u_k$, and $\epsilon = \epsilon_0 - \sum_{k\geq 1} s^k \epsilon_k$ for $|s| << 1$.

The $\mathcal{O}(s)$ equation,

$$\epsilon_0^2 u_1'' + u_1 + \gamma B u_1 = 0, \tag{3.35}$$

has an infinite number of solutions consisting of the space spanned by $cos(n\pi x)$. We will take $u_1 = cos(n\pi x)$, since without loss of generality we can simply rescale s. Collecting the $\mathcal{O}(s^2)$ terms yields the equation,

$$\epsilon_0^2 u_2'' + u_2 + \gamma B u_2 = 2\epsilon_0\epsilon_1 u_1'' = -2\epsilon_0\epsilon_1 n^2\pi^2 cos(n\pi x). \tag{3.36}$$

By the Fredholm alternative, this equation has a solution if and only if the right-hand side is orthogonal to $cos(n\pi x)$, from which we obtain $\epsilon_1 = 0$. With the additional requirement $(u_2, u_1)_0 = 0$ we have $u_2 = 0$. The $\mathcal{O}(s^3)$ equation is

$$\epsilon_0^2 u_3'' + u_3 + \gamma B u_3 = 2\epsilon_0\epsilon_2 u_1'' + u_1^3. \tag{3.37}$$

Expanding the u_1^3 term we obtain

$$2\epsilon_0\epsilon_2 u_1'' + u_1^3 = (\frac{3}{4} - 2\epsilon_0\epsilon_2 n^2\pi^2)cos(n\pi x) + \frac{1}{4}cos(3n\pi x), \tag{3.38}$$

and from the solvability condition we find

$$\epsilon_2 = \frac{3}{8}\frac{1}{n^2\pi^2\epsilon_0}.$$

Therefore, we have

$$u = s\cos(n\pi x) + \mathcal{O}(s^3), \tag{3.39}$$

$$\epsilon = \epsilon_0 - \frac{3}{8}\frac{1}{n^2\pi^2\epsilon_0}s^2 + \mathcal{O}(s^3), \tag{3.40}$$

for $|s|$ sufficiently small.

At the bifurcation value ϵ_0 the zero solution undergoes a pitchfork bifurcation. This bifurcation yields a pair of solutions $m_n^{\pm}$ such that $m_n^- = -m_n^+$ as depicted in Figure 2. When $0 \leq \gamma < 1$, for each mode there is an ϵ value at which a bifurcation

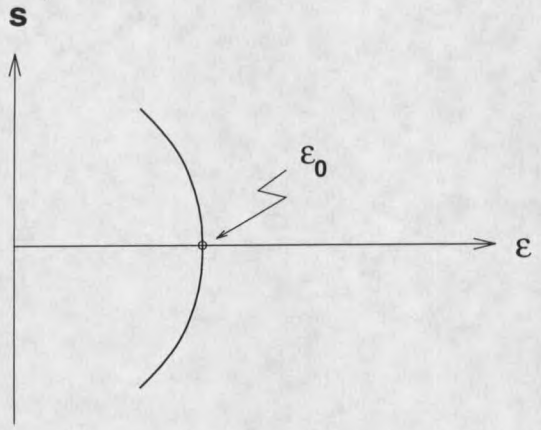


Figure 2: Local solution branch.

occurs. For $\gamma > 1$, not all modal bifurcations occur by varying ϵ unless γ is sufficiently small. In this case, for an n^{th} mode bifurcation to occur with γ fixed we also need $D(n\pi)^2 + 1 > \gamma$. We note that these bifurcations correspond to the so called Turing bifurcations of the system (1.2), (1.3). Figure 3 shows numerical computations of the m_1^+ and m_2^+ solutions computed using AUTO [8] with $\gamma = 0.6$ and $D = 1$. To simplify our analysis, we will take $D = 1$ for the remainder of this thesis.

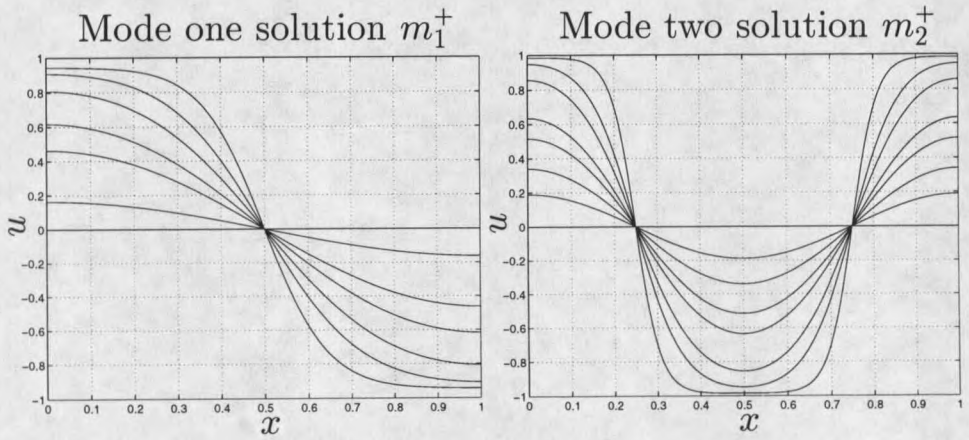


Figure 3: Mode 1 and 2 solutions. Steepening of transition layers occurs as $\epsilon \to 0$.

Stability of the Bifurcating Solutions

To determine the stability of the bifurcating solutions, we consider the eigenvalue problem

$$\epsilon^2\phi'' + f'(u)\phi + \gamma B\phi = \lambda\phi, \quad \phi'(0) = \phi'(1) = 0. \tag{3.41}$$

For the constant solutions, $u = m_0^{\pm}$, we have

$$\lambda_n = -(\epsilon n\pi)^2 + 3\gamma - 2 - \frac{\gamma}{(n\pi)^2 + 1}, \tag{3.42}$$

$$\phi_n(x) = cos(n\pi x), \quad n = 0, 1, \ldots, . \tag{3.43}$$

For the nonconstant solutions the eigenvalue problem cannot be solved in closed form. To analyze the stability in this case, let $\epsilon = \epsilon_0 - s^2\epsilon_2 + \mathcal{O}(s^3)$, $u = su_1 + \mathcal{O}(s^3)$ be the n^{th} mode solution curve previously obtained. Following [31], we will look for λ and ϕ as a power series in s, that is $\lambda = \sum_{i=0}^{\infty} s^i\lambda_i$, $\phi = \sum_{i=0}^{\infty} s^i\phi_i$.

The $\mathcal{O}(1)$ equation is simply the eigenvalue problem

$$\epsilon_0^2\phi_0'' + \phi_0 + \gamma B\phi_0 = \lambda_0\phi_0, \quad \phi_0'(0) = \phi_0'(1) = 0, \tag{3.44}$$

which has the solutions

$$\lambda_{0,k} = \mu_k, \quad \phi_{0,k} = cos(k\pi x), \quad k = 0, 1, 2, \ldots, \tag{3.45}$$

where μ_k is the k^{th} eigenvalue from (3.29) with $\epsilon = \epsilon_0$ and $D = 1$. For $k \neq n$, $\mu_k \neq 0$, and for $|s|$ sufficiently small the stability is determined from the $\mathcal{O}(1)$ term. For the n^{th} eigenvalue we need to determine higher order terms of the expansion.

The $\mathcal{O}(s)$ equation is

$$\epsilon_0^2\phi_{1,n}'' + \phi_{1,n} + \gamma B\phi_{1,n} - \lambda_{0,n}\phi_{1,n} = \lambda_{1,n}\phi_{0,n}. \tag{3.46}$$

By the Fredholm alternative we need the right-hand side of (3.46) orthogonal to $\phi_{0,n}$. Thus, it is clear that we must have $\lambda_{1,n} = 0$ and we will take the solution $\phi_{1,n} = 0$.

The $\mathcal{O}(s^2)$ equation is

$$\epsilon_0^2\phi''_{2,n} + \phi_{2,n} + \gamma B\phi_{2,n} - \lambda_{0,n}\phi_{2,n} = \lambda_{2,n}\phi_{0,n} + 3u_1^2\phi_{0,n} + 2\epsilon_0\epsilon_2\phi''_{0,n}. \tag{3.47}$$

Using the solvability condition and the trigonometric identity $cos^2(n\pi x) = \frac{1}{2}(1 + cos(2n\pi x))$, we have

$$\begin{aligned} \lambda_{2,n} &= -\frac{3}{2} - \frac{3}{2}\frac{(cos(2n\pi x)\phi_{0,n}, \phi_{0,n})_0}{(\phi_{0,n}, \phi_{0,n})_0} + 2(n\pi)^2\epsilon_0\epsilon_2, & (3.48)\\ &= -\frac{3}{2} + 2(n\pi)^2\epsilon_0\epsilon_2, & (3.49)\\ &= -\frac{3}{4}. & (3.50) \end{aligned}$$

Hence, we find for $|s|$ sufficiently small

$$\lambda_n = -\frac{3}{4}s^2 + \mathcal{O}(s^3), \tag{3.51}$$

and this eigenvalue does not contribute to the instability of the solution. Therefore, we see for $|s|$ sufficiently small the dimension of the unstable manifold, or Morse index, is determined by the eigenvalues μ_k for $k \neq n$. Figure 4 summarizes these results for the first five modes and we should devote some time to explaining how to interpret this diagram.

The integer in each of the regions gives the Morse index of the bifurcating solutions which appear as the region is entered by crossing bifurcation curves which comprise the top and right boundaries away from the intersection points. When crossing a top boundary, the solutions are unstable to the modes whose primary bifurcation curves lie directly above that boundary. The solutions which appear by crossing the right boundary are unstable to those modes whose primary curves are directly to the right. We note these results follow from the local analysis and hold only in a sufficiently small neighborhood of the bifurcation curves.

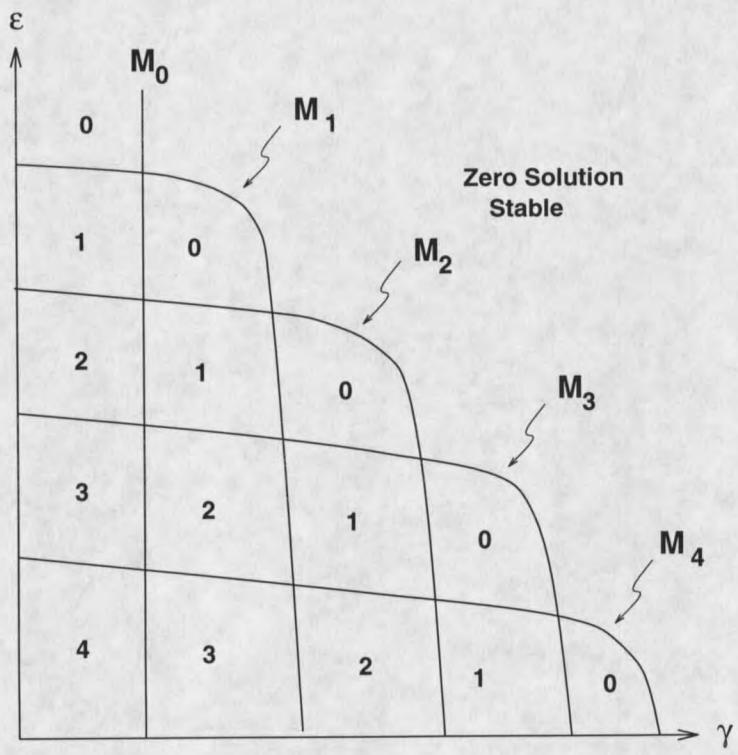


Figure 4: Modal bifurcations from zero and their local Morse index.

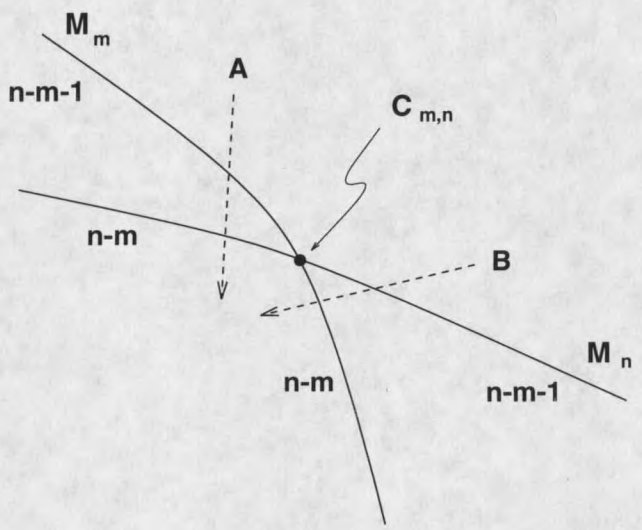


Figure 5: Bifurcation curve intersection point.

Secondary Bifurcations: Lyapunov Schmidt Reduction

As previously mentioned, at the intersection points of the bifurcation curves the operator $\mathcal{L}$ given in (3.28), which corresponds to the linearization about the zero solution, has a two-dimensional null space. This suggests the existence of secondary bifurcations. To see why this is so, consider the intersection of the M_n and M_m bifurcation curves with $n > m$ as shown in Figure 5. As we cross the bifurcation curves in the path given by **A**, the m^{th} mode bifurcates with an $n-m-1$-dimensional unstable manifold, followed by the n^{th} mode which has an $n-m$-dimensional unstable manifold. Moreover, at the latter bifurcation the n^{th} mode solution is unstable to m^{th} mode perturbations. When crossing the bifurcation curves along the path indicated by **B**, the sequence and relative stability are reversed. This suggests there are secondary bifurcation curves which emanate from the point $C_{m,n}$, the crossing of which results in an exchange of stability between these two modes.

To analyze bifurcations that occur near these points we will use the method known as Lyapunov-Schmidt reduction. Excellent presentations of this method can be found in [13] and [31]. Let X and Y be Hilbert spaces and $\mathcal{G} : X \times \mathbb{R}^k$ a smooth mapping with $\mathcal{G}(0,0) = 0$. We wish to solve the equation

$$\mathcal{G}(x, \theta) = 0, \tag{3.52}$$

near $(0,0)$. Assume $L \equiv D_x\mathcal{G}(0,0)$ is a Fredholm operator with index zero. Then X and Y have the following splittings,

$$X = N(L) \oplus M, \tag{3.53}$$

$$Y = S \oplus R(L), \tag{3.54}$$

where M and S are closed subspaces of X and Y, respectively. Let $P : X \to M$ and $Q : Y \to R(L)$ be projection operators associated with these splittings. Then (3.52) can be written as the equivalent pair of equations

$$Q\mathcal{G}(x, \theta) = 0, \tag{3.55}$$

$$(I - Q)\mathcal{G}(x, \theta) = 0. \tag{3.56}$$

Now define $\mathcal{H} : N(L) \times \mathbb{R}^k \times M \to R(L)$ by

$$\mathcal{H}(x_0, \theta, x_1) = Q\mathcal{G}(x_0 + x_1, \theta). \tag{3.57}$$

Then

$$D_{x_1}\mathcal{H}(0,0,0) = QLP \tag{3.58}$$

and since QLP is nonsingular, the implicit function theorem allows us to solve (3.57) for x_1 as a function of x_0 and θ, $x_1 = \Psi(x_0, \theta)$, in a neighborhood of $(0,0)$ in $N(L) \times \mathbb{R}^k$. Substituting this solution into (3.56) we obtain a finite-dimensional system referred to as the bifurcation equations:

$$(I - Q)\mathcal{G}(x_0 + \Psi(x_0, \theta), \theta) = 0. \tag{3.59}$$

The utility of the method comes from the following theorem whose proof can be found in [31].

Theorem 3.5 *In a sufficiently small neighborhood of* $(0,0)$*, solutions to (3.52) are in one-to-one correspondence with solutions of the system (3.59).*

To apply this technique, let $C_{m,n} = (\gamma_0, \epsilon_0)$ be a point of intersection for the m^{th} and n^{th} mode bifurcation curves and define the local stretched coordinates η and ρ in parameter space by

$$\epsilon^2 = \epsilon_0^2 - s^2\eta, \tag{3.60}$$

$$\gamma = \gamma_0 - s^2\rho, \tag{3.61}$$

where $s << 1$. Note this change of coordinates moves the point $C_{m,n}$, to the origin, reflects the plane about the negative identity, and stretches the coordinates. For (γ, ϵ) near (γ_0, ϵ_0) (3.15) becomes

$$\epsilon_0^2 u_{xx} + \gamma_0 Bu + f(u) = s^2\eta u_{xx} + s^2\rho Bu. \tag{3.62}$$

Now assume an odd power series expansion of u

$$u = su_0 + s^3u_1 + \mathcal{O}(s^5). \tag{3.63}$$

Substituting this into (3.62) and equating coefficients of powers of s we find the $\mathcal{O}(s)$ and $\mathcal{O}(s^3)$ equations are:

$$\mathcal{O}(s): \quad \epsilon_0^2 u_0'' + \gamma_0 Bu_0 + u_0 = 0, \tag{3.64}$$

$$\mathcal{O}(s^3): \quad \epsilon_0^2 u_1'' + \gamma_0 Bu_1 + u_1 = \eta u_0'' + \rho Bu_0 + u_0^3. \tag{3.65}$$

Equation (3.64) has an infinite number of solutions given by

$$u_0 = a\cos(m\pi x) + b\cos(n\pi x), \quad a, b \in \mathbb{R}. \tag{3.66}$$

For (3.65), the Fredholm alternative requires the right-hand side to be orthogonal to $span\{cos(m\pi x), cos(n\pi x)\}$ from which we obtain the leading order bifurcation equations

$$-\zeta_m a + g_m(a,b) = 0, \tag{3.67}$$

$$-\zeta_n a + g_n(a,b) = 0 \tag{3.68}$$

where

$$\zeta_k = \eta(k\pi)^2 + \frac{\rho}{(k\pi)^2+1},$$

and

$$g_k(a,b) = \int_0^1 u_0^3 cos(k\pi x)dx.$$

Closed form solutions for (3.67)-(3.68) can be found for all modes, and are as follows:

- Case I: If $m = 0$, then

$$g_0(a,b) = a^3 + \frac{3}{2}ab^2,$$
$$g_n(a,b) = \frac{3}{4}b^3 + 3ab^2,$$

and the solutions are

  - Zero solution: $(a,b) = (0,0)$,
  - Pure m-mode: $a = \pm\sqrt{\zeta_0}, \quad b = 0,$
  - Pure n-mode: $a = 0, \quad b = \pm\sqrt{\frac{4}{3}(\zeta_n)},$
  - Mixed modes:

$$a = \pm\sqrt{\frac{\zeta_n - 2\zeta_0}{5}}, \quad b = \frac{2}{15}\sqrt{45\zeta_0 - 15\zeta_n},$$

$$a = \pm\sqrt{\frac{\zeta_n - 2\zeta_0}{5}}, \quad b = -\frac{2}{15}\sqrt{45\zeta_0 - 15\zeta_n}.$$

- Case II: If $m > 0$, then

$$g_m(a,b) = \frac{3}{4}a^3 + \frac{3}{2}ab^2,$$
$$g_n(a,b) = \frac{3}{4}b^3 + \frac{3}{2}a^2b,$$

and the solutions are

  - Zero solution: $(a,b) = (0,0)$,
  - Pure m-mode: $a = \pm\sqrt{\frac{4}{3}\zeta_m}, \quad b = 0,$
  - Pure n-mode: $a = 0, \quad b = \pm\sqrt{\frac{4}{3}\zeta_n},$
  - Mixed modes:

$$a = \pm\frac{2}{3}\sqrt{2\zeta_n - \zeta_m}, \quad b = \frac{2}{3}\sqrt{2\zeta_m - \zeta_n},$$
$$a = \pm\frac{2}{3}\sqrt{2\zeta_n - \zeta_m}, \quad b = -\frac{2}{3}\sqrt{2\zeta_m - \zeta_n}.$$

From these solutions the local bifurcation curves and the bifurcation diagrams can be easily constructed. A caricature of a set of bifurcation curves in the local parameter space is depicted in Figure 6. There are two primary curves, one for each pure mode solution and a set of secondary bifurcation curves that bound a sector in which the mixed mode solutions exist. The primary curves are given by $\zeta_m = 0$ and $\zeta_n = 0$. The secondary bifurcation curves are as follows:

- Secondary bifurcations from the m-mode solution:
  - Case I: $\zeta_n \geq 2\zeta_0$ and $3\zeta_0 = \zeta_n$
  - Case II: $2\zeta_n \geq \zeta_m$ and $2\zeta_m = \zeta_n$
- Secondary bifurcations from the n-mode solution:
  - Case I: $3\zeta_0 \geq \zeta_n$ and $2\zeta_0 = \zeta_n$

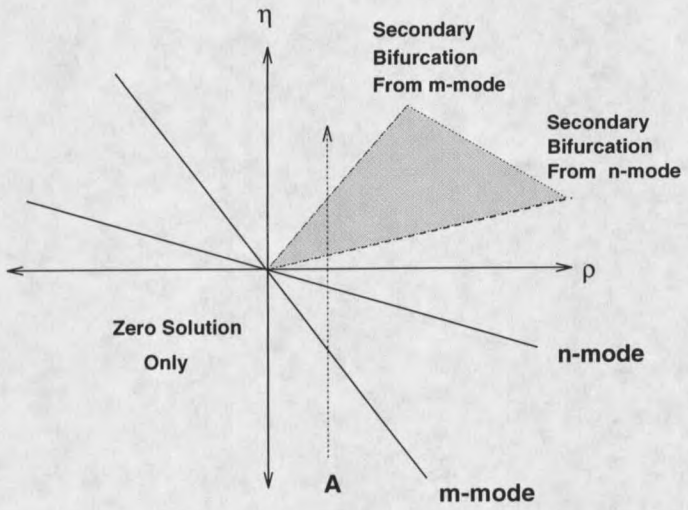


Figure 6: Bifurcation curves in local parameter coordinates.

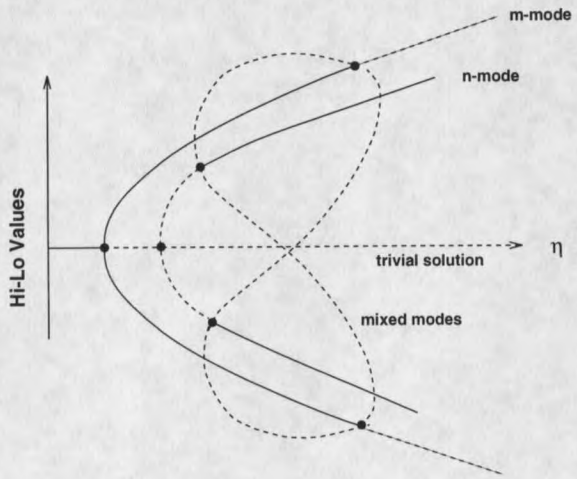


Figure 7: Bifurcation diagram along path **A**.

– Case II: $2\zeta_n \geq \zeta_m$ and $2\zeta_m = \zeta_n$

For the various modes the slope of the bifurcation curves differs but each case gives a qualitatively similar figure. A bifurcation diagram for solutions along the path **A** appears in Figure 7. In this diagram the solutions are represented by their "Hi-Lo Values", which is the sum of their planar (a, b) components. In the diagram we have indicated stability of the solutions as equilibria for the system

$$\frac{da}{dt} = \zeta_m a - g_m(a, b), \tag{3.69}$$

$$\frac{db}{dt} = \zeta_n b - g_n(a, b). \tag{3.70}$$

For the infinite-dimensional system this translates to stability within the linear subspace $span\{cos(m\pi x), cos(n\pi x)\}$.

Proceeding in parameter space along the path **A**, we see first the appearance of the m-mode solutions followed by the pure n-mode solutions. This is then followed by the appearance of mixed mode solutions which bifurcate from the n-modes. These mixed modes then coalesce with the m-mode solutions in a bifurcation of the m-mode branch. The end result is an exchange of stability between the two pure mode solutions branches. Different bifurcation diagrams can be obtained by proceeding along different paths in parameter space. An example for modes 2 and 3 is presented in Figures 8 and 9. The bifurcation diagram was obtained by fixing $\rho = 0.01$ and varying η.

We note that Keener [20] has performed a similar analysis of secondary bifurcations for reaction-diffusion systems using the method of two timing. The two timing method, however, only permits the analysis at the intersection points of consecutive modes. Our work generalizes this result.

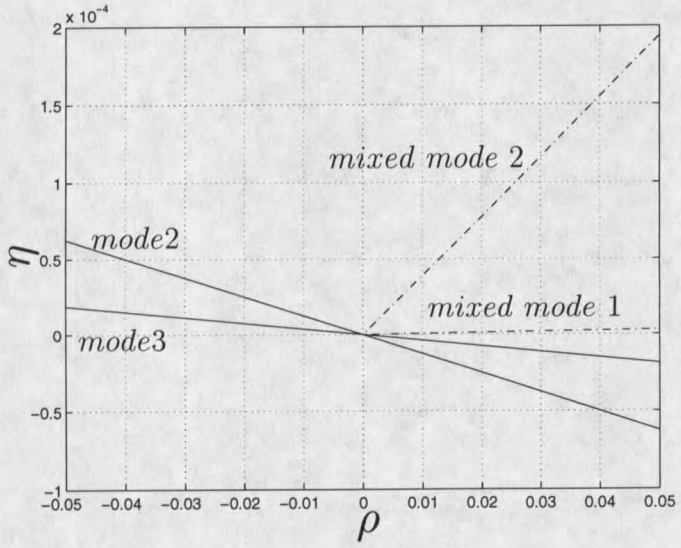


Figure 8: Bifurcation curves for modes 2 and 3 : primary (solid), secondary (- -).

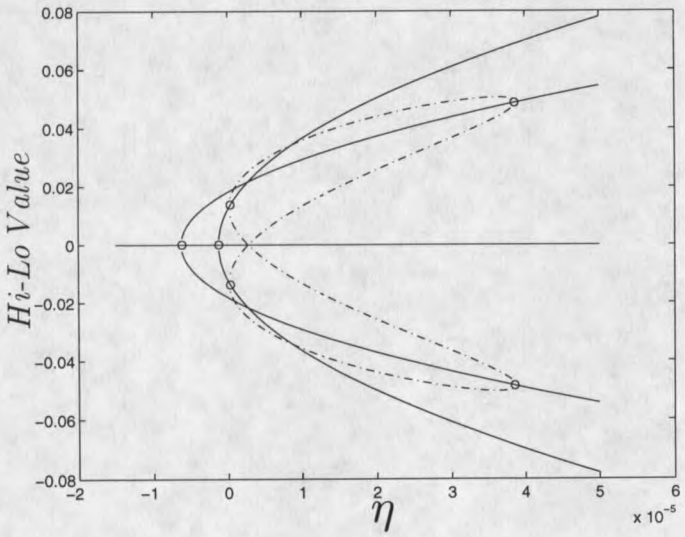


Figure 9: Bifurcation diagram for modes 2 and 3, $\rho = 0.01$: a and b modes (solid), mixed modes (- -).

Bifurcations from the Non-zero Constant Solutions

For the constant solutions, $m_0^{\pm} = \pm\sqrt{1-\gamma}$, the secondary bifurcation curves can be easily computed. From the previous work we saw that the linearization about these equilibria yields the eigenvalues

$$\mu_n = -(\epsilon n\pi)^2 - \frac{\gamma}{D(n\pi)^2+1} - 2 + 3\gamma, \quad n = 0, 1, \ldots. \tag{3.71}$$

Solving $\mu_n = 0$ for ϵ as a function of γ we obtain the family of bifurcation curves

$$\epsilon = \frac{1}{n\pi}\sqrt{\frac{(3\gamma-2)(n\pi)^2 + 2\gamma - 2}{(n\pi)^2+1}}. \tag{3.72}$$

Curves for the first three modes are plotted in Figure 10. One can see that for a judicious choice of ϵ and γ, μ_n is a simple zero eigenvalue and hence a bifurcation occurs by fixing one parameter and allowing the other to vary. The bifurcations are pitchforks and the local solution branches are given by

$$u = m_0^{\pm} + s\cos(n\pi x) + \mathcal{O}(s^2), \tag{3.73}$$

$$\epsilon = \epsilon_0 + \epsilon_2 s^2 + \mathcal{O}(s^3), \quad \epsilon_2 > 0, \tag{3.74}$$

or

$$u = m_0^{\pm} + s\cos(n\pi x) + \mathcal{O}(s^2), \tag{3.75}$$

$$\epsilon = \gamma_0 + \gamma_2 s^2 + \mathcal{O}(s^3), \quad \gamma_2 < 0, \tag{3.76}$$

for $|s|$ sufficiently small. The stability can be analyzed as was done for bifurcations from zero. Moreover, the crossings of these curves suggests possible secondary bifurcations. We will, however, not pursue this investigation at this time.

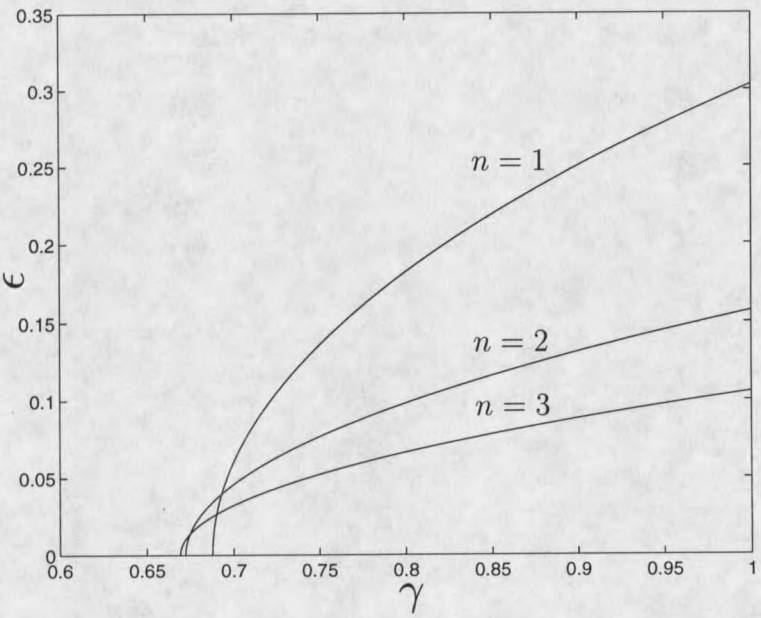


Figure 10: Constant solution bifurcation curves.

CHAPTER 4

INERTIAL MANIFOLDS

Introduction

It is well known that many dissipative infinite-dimensional systems seem to display finite-dimensional behavior. For such systems the attractor is embedded in a finite-dimensional invariant manifold which attracts all solutions at an exponential rate. These manifolds are known as inertial manifolds. If a system possesses an inertial manifold then the long time dynamics are essentially determined by a finite-dimensional system known as the inertial form.

One of the earliest results concerning inertial manifolds for reaction-diffusion systems appears in a paper by Conway, Hoff and Smoller [5]. Their result provides rigorous justification for the "lumped parameter assumption", which states that if the rate of diffusion greatly exceeds the overall reaction rate then the dynamics are essentially determined by the reaction kinetics. Recently, results for inertial manifolds of general evolution equations have been proven. Several references include [12], [29] and [4].

Consider the evolution equation

$$u_t + Au = f(u) \tag{4.1}$$

on a Hilbert space H, where A is a positive self-adjoint operator. The major hypothesis for the existence of an inertial manifold is the existence of a sufficiently large gap in the spectrum of A relative to the Lipschitz constant for the nonlinearity f.

For reaction-diffusion systems this translates into the statement that higher eigenmodes are smoothed by diffusion at a rate which is faster than the overall reaction rate, meaning the higher modes are reaction limited. In proving the existence of an inertial manifold, we look for the manifold as a graph of a function over a finite-dimensional subspace of the Hilbert space H. Specifically, letting P be the projection onto the span of the first N eigenfunctions of A and $Q = I - P$, we construct the manifold as the graph of a function $\Phi : PH \mapsto QH$. If u is a solution to the evolution equation on the inertial manifold then $u = p + \Phi(p)$ where $p \in PH$ satisfies the finite-dimensional system,

$$\frac{dp}{dt} + Ap = Pf(p + \Phi(p)), \tag{4.2}$$

known as the inertial form. Since every solution to the evolution equation approaches a solution of (4.2) exponentially fast, the large time dynamics of the system are essentially finite-dimensional and determined by (4.2).

Although the existence of an inertial manifold may be rather easy to verify, it is not often the case that the mapping Φ can be explicitly found. Therefore, it must be approximated. This leads us to the notion of an approximate inertial manifold. To be precise, an approximate inertial manifold is a finite-dimensional manifold which attracts solutions to a within a thin neighborhood of itself. Approximate inertial manifolds may exist even when the existence of a true inertial manifold is not known.

In this chapter we will verify the existence of both an inertial manifold for (2.7), and a family of approximate inertial manifolds. The approximate inertial manifolds will provide us with finite-dimensional systems of equations which we will use to obtain qualitative approximations of the attractor.

Existence of an Inertial Manifold

The existence of an inertial manifold can been proven by several methods.

Temam [29] provides an existence theorem for a general class of evolution equation when the nonlinearity f is only Lipschitz continuous. Although the theorem allows for a general class of nonlinearities, the spectral gap condition is somewhat restrictive and does not apply to many differential operators, and the result is a manifold which is only Lipschitz continuous. Chow and Lu [4] have proven an existence theorem with a spectral gap condition which is much less restrictive and even allows for operators which are only sectorial. Their theorem requires the nonlinearity to be C^1 and globally Lipschitz, and the resulting manifold has the same smoothness. This may seem to be restrictive, however, for many equations which are dissipative and possess some smoothing , the nonlinearity can be modified to satisfy the hypotheses. The existence result of Chow and Lu is summarized in the following theorem.

Theorem 4.1 *Let A be a sectorial operator on a Hilbert space H, $0 < \alpha < 1$, and $f \in C^1(D(A^\alpha), H)$ a globally Lipschitz continuous function such that the evolution equation*

$$u_t + Au = f(u), \quad u(0) = u_0 \in D(A^\alpha) \tag{4.3}$$

generates a C^1 semigroup on $D(A^\alpha)$. Assume μ, η are positive constants so that $\sigma(A) = \Sigma_1 \cup \Sigma_2$ where

$$\Sigma_1 = \{\lambda \in \sigma(A) : Re\lambda \leq \mu - \eta\},$$

$$\Sigma_2 = \{\lambda \in \sigma(A) : Re\lambda \geq \mu + \eta\}.$$

Let P be the projection onto to the span of the eigenfunctions associated with Σ_1, $Q = I - P$ and A_1, A_2 the restriction of A to the spaces PH and QH respectively. Also, assume there exist constants M_1, M_2 and N_α such that the following estimates hold:

$$||e^{-A_1 t}P|| \leq M_1 e^{-(\mu-\eta)t}, \quad \forall t \leq 0,$$

$$||e^{-A_2 t}Q|| \leq M_2 e^{-(\mu+\eta)t}, \quad \forall t \geq 0,$$

$$||e^{-A_2 t}Qy||_{D(A^\alpha)} \leq N_\alpha t^{-\alpha} e^{-(\mu+\eta)t}||y||_H, \quad \forall t > 0.$$

If the **spectral gap condition**,

$$Lip(f)\left[\frac{M_1 + M_2}{\eta} + \frac{2-\alpha}{1-\alpha}N_\alpha \eta^{\alpha-1}\right] < 1$$

holds, then the evolution equation has an inertial manifold which is the graph of C^1 *map* $\Phi : PH \to QH$.

Proof: See [4]. □

The hypotheses of the theorem are relatively simple to check, however, (2.7) must be slightly modified since f is not globally Lipschitz. It can be shown for $\gamma > 0$ the unit ball in $C[0,1]$ is an absorbing set. That is, all solutions enter this ball in finite time. Let θ be a C^∞ function such that $\theta(s) = 1$ if $0 \leq s \leq 1$ and $\theta(s) = 0$ if $s \geq 2$. Define $F : \mathbb{R} \to \mathbb{R}$ by

$$F(s) = \theta(s^2)f(s).$$

Then F is C^1 and there exist constants C_F and $C_{F'}$ such that

$$|F(s)| \leq C_F, \quad \forall s \in \mathbb{R}, \tag{4.4}$$

$$|F'(s)| \leq C_{F'}, \quad \forall s \in \mathbb{R}. \tag{4.5}$$

Therefore, considered as a mapping, $F : D(A^{1/2}) \to L^2(0,1)$, F is C^1, globally bounded and globally Lipschitz with

$$||F(u)||_0 \leq C_F, \quad \forall u \in D(A^{1/2}), \tag{4.6}$$

$$||F'(u)||_0 \leq C_{F'}, \quad \forall u \in D(A^{1/2}), \tag{4.7}$$

$$||F(u) - F(v)||_0 \leq C_{F'}||u - v||_0, \quad \forall u, v \in D(A^{1/2}). \tag{4.8}$$

By Lemma 2.2

$$C_{F'}||u - v||_0 \leq \frac{C_{F'}}{\sqrt{\sigma_p}}||u - v||_1 \equiv Lip(F)||u - v||_1. \tag{4.9}$$

Therefore, F satisfies the hypothesis of the theorem. Moreover, F restricted to the absorbing set is f . Thus, in the absorbing set (2.7) agrees with the modified equation

$$u_t + Au = F(u). \tag{4.10}$$

The unit ball in $C[0,1]$ is an absorbing ball for the modified equation hence the large time behavior of the equations is the same. The following lemma, proven in [16], will provide us the necessary estimates on the semigroup e^{-At}.

Lemma 4.2 *Let A be a sectorial operator, Σ_1 be a finite collection of eigenvalues of A, $\Sigma_2 = \sigma(A) - \Sigma_1$ and let E_1 and E_2 be the the associated eigenspaces. Let A_1 and A_2 denote the restriction of A to E_1 and E_2, respectively.*

1. *If $Re\Sigma_1 < \alpha$ then $||e^{-A_1 t}|| \leq Me^{-\alpha t}$ for $t < 0$,*
2. *If $Re\Sigma_2 > \beta$, then for $t > 0$, $||e^{-A_2 t}|| \leq Me^{-\beta t}$, and $||A_2 e^{-A_2 t}|| \leq Mt^{-1}e^{-\beta t}$.*

Taking $\Sigma_1 = \{\sigma_0, \ldots, \sigma_N\}$, $\mu = \frac{\sigma_N + \sigma_{N+1}}{2}$ and $\eta = \frac{\sigma_{N+1} - \sigma_N}{2}$ the estimates on e^{-At} hold and the spectral gap condition of Theorem 4.1 is satisfied by taking N sufficiently large. We have verified the following result:

Theorem 4.3 *The nonlocal reaction-diffusion equation (4.10) possesses an inertial manifold which is the graph of a C^1 mapping $\Phi : PH \to QH$.*

Like center manifolds for finite-dimensional systems, inertial manifolds are not necessarily unique. The theorem only guarantees the existence and provides extremely poor estimates of a minimal dimension. We would expect there exists a well defined inertial manifold having dimension close to that of the attractor. In fact, it has been shown for some scalar reaction-diffusion equations that there is an inertial manifold having the same dimension as the attractor and the manifold can be explicitly constructed [18]. This result, however, requires a priori knowledge of the structure of the attractor which we do not have for (4.10).

The following result, which is in the spirit of [5], tells us that when ϵ is large the attractor and inertial manifold of (4.10) are very simple and we can obtain an explicit representation.

Theorem 4.4 *For ϵ sufficiently large, the solution $u(t)$ of (4.10) satisfies*

$$||u(t) - \bar{u}(t)||_0 \leq C_1 e^{-\sigma t} \tag{4.11}$$

where C_1 and σ are positive constants and $\bar{u}(t)$ satisfies

$$\frac{d\bar{u}}{dt} = -\gamma\bar{u} + F(\bar{u}) + \mathcal{O}(e^{-\sigma t}), \quad \bar{u}(0) = \int_0^1 u(0)dx \tag{4.12}$$

Proof: Let $\bar{u}(t) = \int_0^1 u(x,t)dx$. Then $\bar{u}$ satisfies

$$\frac{d\bar{u}}{dt} = -\gamma\bar{u} + F(\bar{u}) + \int_0^1 \left(F(u) - F(\bar{u})\right) dx. \tag{4.13}$$

Therefore

$$\begin{aligned}
\frac{1}{2}\frac{d}{dt}||u-\bar{u}||_0^2 &= -||A^{1/2}(u-\bar{u})||_0^2 + (u-\bar{u}, F(u)-F(\bar{u}))_0 \\
&\quad + \left(\int_0^1 u - \bar{u}dx\right)\left(\int_0^1 F(u) - F(\bar{u})dx\right), \\
&\leq -\bar{\sigma}||u-\bar{u}||_0^2 + ||u-\bar{u}||_0||F(u)-F(\bar{u})||_0, \\
&\leq (-\bar{\sigma} + C_{F'})||u-\bar{u}||_0^2,
\end{aligned}$$

where $\bar{\sigma}$ is the principle eigenvalue of A restricted to the subspace of functions having zero mean. Choosing ϵ sufficiently large that $-\bar{\sigma} + C_{F'} < 0$, we have

$$||u-\bar{u}||_0^2 \leq ||u(0)-\bar{u}(0)||_0^2 e^{2(-\bar{\sigma}+C_{F'})t}. \tag{4.14}$$

This estimate along with the Lipschitz continuity of F shows that $\bar{u}$ satisfies

$$\frac{d\bar{u}}{dt} = -\gamma\bar{u} + F(\bar{u}) + \mathcal{O}(e^{-\sigma t}). \tag{4.15}$$

□

In this parameter regime the attractor and inertial manifold are identical and are in

fact one-dimensional. The large time behavior of solutions is essentially determined by the ordinary differential equation

$$\frac{du}{dt} = f(u) - \gamma u.$$

Approximate Inertial Manifolds

The existence proof for the inertial manifold discussed in the previous section does not provide insight into a practical approach for approximating the manifold. Moreover, as we previously mentioned, the theorem yields a manifold of rather large dimension. For example, if $\gamma = 1$ and $\epsilon = 0.5$, then Theorem 4.4 applies and the inertial manifold is one-dimensional. However, to satisfy the spectral gap condition of Theorem 4.1 we need $N \geq 49$. Thus, we see the manifold constructed in the existence theorem does not provide a reasonable computational tool.

In this section, we prove the existence of a low-dimensional manifold which contains the equilibria and attracts all solutions to a neighborhood of itself. This manifold, which is referred to as a steady inertial manifold, is relatively straightforward to approximate, and estimates of its dimension are easily obtained. Approximations of the manifold will provide us with approximate inertial forms which can be computationally implemented. Our approach follows the method outlined in [19] and numerically examined in [26]. However, due to our modified function F, we are able to define the manifold used in our work in $L^2(0,1)$, rather than in $D(A^{1/2})$ as is done in [19] and [26]. The result is a manifold of smaller dimension.

Let P be the projection onto $span\{\phi_0, \ldots, \phi_{N-1}\}$, and $Q = I - P$. Define $\lambda = max\{\sigma_0, \sigma_1, \ldots, \sigma_{N-1}\}$ and $\Lambda = min\{\sigma_N, \sigma_{N+1}, \ldots\}$. Let $\mathcal{B}$ be a closed ball centered at zero in $QL^2(0,1)$ of radius greater than $\frac{C_F}{\Lambda}$. For $p \in PL^2(0,1)$ define

$T_p : \mathcal{B} \to QL^2(0,1)$ by

$$T_p(q) = A^{-1}QF(p+q). \tag{4.16}$$

By (4.4) and (4.5), F considered as a function from $L^2(0,1)$ to $L^2(0,1)$ is Lipschitz continuous with Lipschitz constant $C_{F'}$. Therefore, the mapping T_p is well defined and is as smooth as the function F. In this case it is at least C^1. To analyze this mapping , we will need the following lemma:

Lemma 4.5 *Let P, Q, λ and Λ be as previously defined. Then for all $\beta \in \mathbb{R}$ the following inequalities hold:*

$$||A^{\beta+1/2}p||_0^2 \leq \lambda ||A^{\beta}p||_0^2, \quad \forall p \in PD(A^{\beta}) \cap PD(A^{\beta+1/2}), \tag{4.17}$$

$$||A^{\beta+1/2}q||_0^2 \geq \Lambda ||A^{\beta}q||_0^2, \quad \forall q \in QD(A^{\beta}) \cap PD(A^{\beta+1/2}). \tag{4.18}$$

Proof: Let $p \in PD(A^{\beta})$, then $p = \sum_{n=0}^{N-1} p_n \phi_n(x)$ and $A^{\beta+1/2}p = \sum_{n=0}^{N-1} \sigma_n^{\beta+1/2} p_n \phi_n(x)$. Therefore

$$||A^{\beta+1/2}p||_0^2 = \sum_{n=0}^{N-1} \sigma_n^{2\beta+1} p_n^2 \leq \lambda \sum_{n=0}^{N-1} \sigma_n^{2\beta} p_n^2 = \lambda ||A^{\beta}p||_0^2. \tag{4.19}$$

and (4.17) is true. To see (4.18), let $q \in QD(A^{\beta})$, then $q = \sum_{n=N}^{\infty} q_n \phi_n(x)$ and $A^{\beta+1/2}q = \sum_{n=N}^{\infty} \sigma_n^{\beta+1/2} q_n \phi_n(x)$. Therefore

$$||A^{\beta+1/2}q||_0^2 = \sum_{n=N}^{\infty} \sigma_n^{2\beta+1} q_n^2 \geq \Lambda \sum_{n=N}^{\infty} \sigma_n^{2\beta} q_n^2 = \Lambda ||A^{\beta}q||_0^2. \tag{4.20}$$

■

We are now ready to prove the following theorem.

Theorem 4.6 *If N is sufficiently large that $C_{F'} < \Lambda$, then there is an N-dimensional manifold $\mathcal{M}^s$ which is the graph of a C^1 mapping $\Phi^s : PL^2(0,1) \to QL^2(0,1)$ and contains the equilibria for (4.10).*

Proof: From Lemma 4.5 we have

$$||T_p(q)||_0 = ||A^{-1}QF(p+q)||_0 \leq \frac{||F(p+q)||_0}{\Lambda} \leq \frac{C_F}{\Lambda}, \tag{4.21}$$

and therefore, $T_p : \mathcal{B} \to \mathcal{B}$ for all $p \in PL^2(0,1)$. Now for $q_1, q_2 \in \mathcal{B}$,

$$||T_p(q_1) - T_p(q_2)||_0 = ||A^{-1}Q(F(p+q_1) - F(p+q_2))||_0, \tag{4.22}$$

$$\leq \frac{C_{F'}}{\Lambda}||q_1 - q_2||_0, \tag{4.23}$$

and for N sufficiently large, T_p is a contraction on $\mathcal{B}$ which is uniform in p. Therefore, by the uniform contraction mapping theorem (see [3]), for each $p \in PL^2(0,1)$, T_p has a unique fixed point $q(p) \in \mathcal{B}$. Moreover, the map $\Phi^s : PL^2(0,1) \to \mathcal{B}$ which takes p to the corresponding fixed point, is C^1 and the graph of Φ^s defines an N-dimensional manifold, $\mathcal{M}^s$, over $PL^2(0,1)$. Now let u be an equilibrium solution of (4.10). Then $u = p + q$ where

$$Ap = PF(p+q), \tag{4.24}$$

$$Aq = QF(p+q). \tag{4.25}$$

But $q = A^{-1}QF(p+q) = T_p(q)$, meaning q is the unique fixed point of T_p and $q = \Phi^s(p)$. Hence, $\mathcal{M}^s$ contains the equilibria for (4.10). ■

Dimension of $\mathcal{M}^s$	$\gamma = 0.25$	$\gamma = 0.5$	$\gamma = 0.75$	$\gamma = 1$	$\gamma = 1.5$	$\gamma = 2$
N	$\epsilon >$	$\epsilon >$	$\epsilon >$	$\epsilon >$	$\epsilon >$	$\epsilon >$
1	0.4476	0.4449	0.4423	0.4439	0.4344	0.4289
2	0.2247	0.2243	0.2240	0.2236	0.2229	0.2223
3	0.1499	0.1498	0.1497	0.1496	0.1494	0.1492
4	0.1125	0.1125	0.1124	0.1124	0.1123	0.1122
5	0.0901	0.0900	0.0899	0.0899	0.8989	0.08985

Table 1: Dimension estimates for $\mathcal{M}^s$ in $L^2(0,1)$.

Although we cannot explicitly compute this manifold, we can easily obtain estimates of its dimension and it can be approximated by a sequence of manifolds which can be computed. Dimensional estimates for $\mathcal{M}^s$ based on the contraction condition,

$\Lambda \geq C_{F'}$, using the value $C_{F'} = 2$ are listed in Table 1. To obtain approximations of the function Φ^s, define

$$\Phi_0(p) = 0, \quad \forall p \in PL^2(0,1), \tag{4.26}$$

and

$$\Phi_{k+1}(p) = T_p(\Phi_k(p)), \quad \forall p \in PL^2(0,1), \quad k = 0, 1, 2, \ldots. \tag{4.27}$$

We will show these functions converge to Φ^s and provide error estimates. First note that

$$||\Phi_1(p)||_0 = ||A^{-1}QF(p)||_0 \leq \frac{C_F}{\Lambda}.$$

Let $\Xi = \frac{C_{F'}}{\Lambda}$. Then

$$||\Phi_{k+1}(p) - \Phi_k(p)||_0 \leq \Xi^k ||\Phi_1(p) - \Phi_0(p)||_0 = \Xi^k ||\Phi_1(p)||_0, \tag{4.28}$$

so

$$||\Phi_{k+1}(p) - \Phi_k(p)||_0 \leq \Xi^k \frac{C_F}{\Lambda} \tag{4.29}$$

and the sequence $\{\Phi_k(p)\}$ is Cauchy. Let $\bar{q}$ be the limit. Since T_p is continuous

$$\lim_{k \to \infty} T_p(\Phi_k(p)) = T_p(\bar{q}) \tag{4.30}$$

and

$$\bar{q} = T_p(\bar{q}). \tag{4.31}$$

Therefore, $\Phi_k(p) \to \Phi^s(p)$ and the convergence is uniform in p. Now, since

$$\Phi^s(p) - \Phi_k(p) = \sum_{n=k}^{\infty} [\Phi_{k+1}(p) - \Phi_k(p)] \tag{4.32}$$

we have the uniform error estimate

$$||\Phi^s(p) - \Phi_k(p)||_0 \leq \sum_{n=k}^{\infty} \Xi^n ||\Phi_1(p)||_0 \leq \frac{\Xi^k C_F}{\Lambda(1-\Xi)}. \tag{4.33}$$

The steady inertial manifold, $\mathcal{M}^s$, corresponds to a quasi-steady state assumption on the higher modes. That is, if $u = p + q$ is a solution of the evolution equation with

$$p_t + Ap = PF(p + q), \tag{4.34}$$

$$q_t + Aq = QF(p + q), \tag{4.35}$$

then under the assumption $q_t = 0$ we obtain the equations restricted to $\mathcal{M}^s$

$$p_t = -Ap + PF(p + \Phi^s(p)). \tag{4.36}$$

Using functions Φ_k, we define nonlinear spectral Galerkin schemes

$$p_t = -Ap + PF(p + \Phi_k(p)), \tag{4.37}$$

for the evolution equation. The case $k = 0$ is the standard Galerkin spectral method, for $k > 1$ we have a Galerkin spectral method with nonlinear correction. Marion [21], has derived the case $k = 1$ for scalar reaction-diffusion equations from purely heuristic arguments. At equilibria (4.36) is exact and using (4.37) seems to be a reasonable approach for approximating equilibria and their bifurcations. However, the use of it to approximate the dynamic behavior of (4.10) near the attractor needs further justification. We will consider only the cases $k = 0$ and $k = 1$ which we will use in later results. We will refer to these systems as AIM-0 and AIM-1 respectively.

Let $u = p + q$ be a solution to (4.10) on the attractor. Then for AIM-0 we have

$$||\Phi_0(p) - q||_0 = ||q||_0. \tag{4.38}$$

For AIM-1 note that

$$A\Phi_1(p) - Aq = QF(p) - QF(p + q) + q_t \tag{4.39}$$

and therefore

$$||A\Phi_1(p) - Aq||_0 \leq ||QF(p) - QF(p+q)||_0 + ||q_t||_0, \tag{4.40}$$

$$\leq C_{F'}||q||_0 + ||q_t||_0. \tag{4.41}$$

Thus by Lemma 4.5 we have

$$||\Phi_1(p) - q||_0 \leq \frac{C_{F'}}{\Lambda}||q||_0 + \frac{1}{\Lambda}||q_t||_0. \tag{4.42}$$

We now need to obtain estimates of $||q||_0$ and $||q_t||_0$.

Lemma 4.7 *Let $u = p + q$ be a solution of the evolution equation (4.10) where $p \in PH$ and $q \in QH$, and let $\delta > 0$. Then there exists a $t^* > 0$ depending on $u(0)$ and δ such that for all $t > t^*$*

$$||q(t)||_0^2 \leq \frac{C_F^2 + \delta}{\Lambda^2}, \quad \textit{and} \quad ||q(t)||_1^2 \leq \frac{C_F^2 + \delta}{\Lambda}. \tag{4.43}$$

Proof: Multiplying

$$q_t + Aq = QF(p+q) \tag{4.44}$$

by Aq and integrating yields

$$\frac{1}{2}\frac{d}{dt}||q||_1^2 + ||Aq||_0^2 = (Aq, F(p+q))_0, \tag{4.45}$$

$$\leq ||Aq||_0||F(p+q)||_0, \tag{4.46}$$

$$\leq ||Aq||_0 C_F, \tag{4.47}$$

$$\leq \frac{1}{2}||Aq||_0^2 + \frac{1}{2}C_F^2. \tag{4.48}$$

Therefore,

$$\frac{d}{dt}||q||_1^2 + ||Aq||_0^2 \leq C_F^2, \tag{4.49}$$

and

$$\frac{d}{dt}||q||_1^2 + \Lambda||q||_1^2 \leq C_F^2. \tag{4.50}$$

Thus by integrating we have

$$||q(t)||_1^2 \leq ||q(0)||_1^2 e^{-\Lambda t} + \frac{C_F^2}{\Lambda}(1 - e^{-\Lambda t}). \tag{4.51}$$

So for t^* sufficiently large we have the second inequality. The first inequality follows from Lemma 4.5. ∎

To obtain an estimate of $||q_t(t)||_0$ we will need the following uniform Gronwall lemma whose proof can be found in [29].

Lemma 4.8 *Let g, h and y be positive locally integrable functions on some interval (t_0, ∞) which satisfy*

$$\frac{dy}{dt} \leq gy + h, \quad t \geq t_0 \tag{4.52}$$

$$\int_t^{t+r} g(s)ds \leq a_1, \quad \int_t^{t+r} h(s)ds \leq a_2, \quad \int_t^{t+r} y(s)ds \leq a_3, \quad t \geq t_0, \tag{4.53}$$

where a_1, a_2, a_3 and r are positive constants. Then

$$y(t+r) \leq \left(\frac{a_3}{r} + a_2\right) e^{a_1}, \quad t \geq t_0. \tag{4.54}$$

Lemma 4.9 *There exists a constant k_2 such that for each $\eta > 0$ there exists a T so that for all $t > T$*

$$||q_t(t)||_0^2 \leq \frac{C_{F'} k_2 + \eta}{\Lambda^2}. \tag{4.55}$$

Proof: Recall from Chapter 2 that for any $k_1 > \frac{1}{2}$ the ball $B_{k_1}(0) \subset D(A^{1/2})$ is absorbing. Now multiplying

$$u_t + Au = F(u)$$

by Au and integrating we have

$$\begin{aligned} \frac{1}{2}\frac{d}{dt}||u||_1^2 + ||Au||_0^2 &= (Au, F(u))_0, & (4.56)\\ &\leq C_F||Au||_0, & (4.57)\\ &\leq \frac{C_F^2}{2} + \frac{1}{2}||Au||_0^2, & (4.58) \end{aligned}$$

and thus

$$\frac{d}{dt}||u||_1^2 + ||Au||_0^2 \leq C_F^2, \tag{4.59}$$

which upon integrating yields

$$||u(t+r)||_1^2 - ||u(t)||_1^2 + \int_t^{t+r} ||Au||_0^2 ds \leq rC_F^2. \tag{4.60}$$

Hence,

$$\int_t^{t+r} ||Au||_0^2 ds \leq rC_F^2 + ||u(t)||_1^2, \tag{4.61}$$

and for t sufficiently large

$$\int_t^{t+r} ||Au||_0^2 ds \leq rC_F^2 + k_1^2. \tag{4.62}$$

Therefore,

$$\int_t^{t+r} ||u_t||_0^2 ds \leq \int_t^{t+r} ||F(u)||_0^2 + 2||F(u)||_0||Au||_0 + ||Au||_0^2 ds. \tag{4.63}$$

Now from the Cauchy-Schwartz inequality we have

$$\int_t^{t+r} ||Au||_0 ds \leq \left(r\int_t^{t+r} ||Au||_0^2 ds\right)^{1/2} \leq \sqrt{r(rC_F^2 + k_1^2)} \tag{4.64}$$

and thus

$$\begin{aligned} \int_t^{t+r} ||u_t||_0^2 ds &\leq rC_F^2 + 2C_F\sqrt{r(rC_F^2 + k_1^2)} + rC_F^2 + k_1^2, & (4.65)\\ &\leq 4rC_F^2 + 2C_F k_1\sqrt{r} + k_1^2. & (4.66) \end{aligned}$$

Now differentiating

$$u_t + Au = F(u), \tag{4.67}$$

with respect to t, multiplying by u_t and integrating we have

$$\frac{1}{2}\frac{d}{dt}||u_t||_0^2 + ||u_t||_1^2 = (F'(u)u_t, u_t)_0, \tag{4.68}$$

$$\frac{1}{2}\frac{d}{dt}||u_t||_0^2 + \sigma_p||u_t||_0^2 \leq C_{F'}||u_t||_0^2, \tag{4.69}$$

$$\frac{d}{dt}||u_t||_0^2 + \leq 2(C_{F'} - \sigma_p)||u_t||_0^2 + \delta. \tag{4.70}$$

By the uniform Gronwall lemma it follows that

$$||u_t(t+r)||_0^2 \leq (4C_F^2 + \frac{2C_F k_1}{\sqrt{r}} + \frac{k_1^2}{r} + \delta r)e^{2(C_{F'} - \sigma_p)r} \tag{4.71}$$

for t sufficiently large and $\delta > 0$ arbitrary. Fix r such that the right-hand side is minimized then set

$$k_2 = \min\{(4C_F^2 + \frac{2C_F k_1}{\sqrt{r}} + \frac{k_1^2}{r}\delta r)e^{2C_{F'}r}\}. \tag{4.72}$$

Differentiating

$$q_t + Aq = QF(u) \tag{4.73}$$

with respect to t and multiplying by q_t and integrating we have

$$\begin{aligned}
\frac{1}{2}\frac{d}{dt}||q_t||_0^2 + ||q_t||_1^2 &= (F'(u)u_t, q_t)_0, && (4.74)\\
&\leq ||F'(u)u_t||_0||q_t||_0, && (4.75)\\
&\leq ||F'(u)u_t||_0\frac{||q_t||_1}{\sqrt{\Lambda}}, && (4.76)\\
&\leq \frac{||F'(u)u_t||_0^2}{2\Lambda} + \frac{1}{2}||q_t||_1^2. && (4.77)
\end{aligned}$$

So now

$$\frac{d}{dt}||q_t||_0^2 + \Lambda||q_t||_0^2 \leq \frac{||F'(u)||_0^2||u_t||_0^2}{\Lambda} \leq \frac{C_{F'}^2 k_2}{\Lambda}, \tag{4.78}$$

and integrating from t^* to t we have

$$||q_t(t)||_0^2 \leq ||q_t(t^*)||_0^2 e^{-\Lambda(t-t^*)} + \frac{C_{F'}^2 k_2}{\Lambda^2}(1 - e^{-\Lambda(t-t^*)}). \tag{4.79}$$

Thus for $\eta > 0$ there exists a T depending on η and $u(0)$ such that for $t > T$ sufficiently large we have

$$||q_t(t)||_0^2 \leq \frac{(C_{F'}^2 k_2 + \eta)}{\Lambda^2}. \tag{4.80}$$

■

From these estimates we see the solutions for AIM-0 are within an $\mathcal{O}(\frac{1}{\Lambda})$ neighborhood of the attractor for Λ large, while the AIM-1 solutions are contained within an $\mathcal{O}(\frac{1}{\Lambda^2})$ neighborhood. The quasi-steady state assumption seems to be reasonable provided Λ is large.

CHAPTER 5

APPROXIMATION OF THE ATTRACTOR

Introduction

In this chapter, we provide numerical evidence for a characterization of a subset of the global attractor. Our main tools will be the approximate inertial manifolds of the previous chapter and simulations based on standard numerical methods. The approximate inertial manifolds provide us with low-dimensional approximations which will allow us to extend the local bifurcation phenomena to a larger region in parameter space and obtain a qualitative picture of the orbits which connect the equilibria. As in previous work, let $\{\sigma_n\}_{n=0}^{\infty}$ denote the eigenvalues of A which are given by (2.8). We will focus our efforts on the region of parameter space,

$$\mathcal{U} = \{(\gamma,\epsilon) \in \mathbb{R}^2 : \sigma_n > 1, \quad n \geq 1\} \cup \{(\gamma,\epsilon) \in \mathbb{R}^2 : \sigma_2 > 2, \quad 0 \leq \gamma \leq \gamma_c\} \tag{5.1}$$

where $\gamma_c = \frac{2}{3}\frac{(\pi^2+1)(4\pi^2+1)}{5\pi^2+1}$ is the intersection point of the mode-one bifurcation curve, M_1, and the curve $\Gamma_s = \{(\gamma,\epsilon) : \sigma_2 = 2\}$. The first subset of the union in (5.1) is the region in which no modal bifurcations from zero occur. In the second subset, the steady approximate inertial manifold , $\mathcal{M}^s$, is two-dimensional and given as the graph of a mapping, Φ^s, over $span\{1, cos(\pi x)\}$. We suspect that in this parameter regime the attractor is also at most two-dimensional. We will use the AIM-0 and AIM-1 approximate inertial forms

$$\frac{du_0}{dt} = -\sigma_0 u_0 + \int_0^1 f(p + \Phi_k^s(p,\epsilon,\gamma))dx, \tag{5.2}$$

$$\frac{du_1}{dt} = -\sigma_1 u_1 + \int_0^1 f(p + \Phi_k^s(p,\epsilon,\gamma))cos(\pi x)dx, \tag{5.3}$$

$k = 0, 1$, where $p = u_0 + u_1 cos(\pi x)$, and

$$\Phi_0 \equiv 0, \tag{5.4}$$

$$\Phi_1(p, \epsilon, \gamma) \equiv A^{-1} Qf(p) = -\frac{3}{2}\frac{u_1^2 u_0}{\sigma_2} cos(2\pi x) - \frac{u_1^3}{4\sigma_3} cos(3\pi x). \tag{5.5}$$

Our strategy will be to characterize the attractor for these systems, then provide independent numerical evidence for a qualitatively similar structure in the attractor for (2.7).

Bifurcation Results

In Chapter 3, we saw that the intersection points of the primary bifurcation curves gave rise to secondary bifurcations. Using the method of Lyapunov-Schmidt Reduction we found that for parameter values sufficiently close to an intersection point the equilibria are contained in a finite-dimensional manifold which is the graph of a function Ψ. This is only a local result and provides no information concerning bifurcations far from the intersection points. However, for parameter values in $\mathcal{U}$, the steady state equations on $\mathcal{M}^s$ provide us with an extension to all of $\mathcal{U}$ of the Lyapunov-Schmidt bifurcation equations obtained at the intersection point, $C_{0,1}$, of the M_0 and M_1 curves. The objective of this section is to provide evidence that the bifurcation structure obtained by the local analysis extends to the region $\mathcal{U}$.

We have already seen that the secondary bifurcation curve for the constant solutions, which will be denoted by Γ_0, does extend globally and is given by

$$\epsilon = \frac{1}{\pi}\sqrt{\frac{(3\gamma - 2)\pi^2 + 2\gamma - 2}{\pi^2 + 1}}, \quad \gamma \leq 1. \tag{5.6}$$

An explicit representation for the curve of secondary bifurcations from the mode-one solutions, which we will denote by Γ_1, cannot be obtained. We conjecture that it does continue globally in $\mathcal{U}$ by the following reasoning. Consider the mode-one

bifurcation occuring for ϵ fixed and $\gamma > 1$. At the bifurcation, the mode-one solution is stable. Now the solution depends continuously on γ , and for $\gamma << 1$ it is unstable. Therefore, a change of stability occurs as γ is decreased which is indicative of a bifurcation. Moreover, this holds for ϵ values away from the point $C_{0,1}$ and thus the phenomena does not appear to be strictly local.

To approximate the curve Γ_1 and obtain a picture of the global bifurcation structure in $\mathcal{U}$, we will use the approximate inertial manifolds and the software package AUTO [8]. The AIM-0 equations are

$$\frac{du_0}{dt} = -\sigma_0 u_0 + u_0 - u_0^3 - \frac{3}{2}u_0 u_1^2, \tag{5.7}$$

$$\frac{du_1}{dt} = -\sigma_1 u_1 + u_1 - \frac{3}{4}u_1^3 - 3u_0^2 u_1. \tag{5.8}$$

All equilibria for this system can be found in closed form and the mode-one solutions are given by

$$(u_0, u_1) = \left(0, \pm\sqrt{\frac{4}{3}(1-\sigma_1)}\right). \tag{5.9}$$

The eigenvalues for linearization about the solutions (5.9) are

$$\lambda_1 = -\sigma_0 - 1 + 2\sigma_1, \tag{5.10}$$

$$\lambda_2 = 2(\sigma_1 - 1). \tag{5.11}$$

The second eigenvalue, λ_2, is negative whenever the mode-one solution exists and is not critical. The first eigenvalue corresponds to stability with respect to constant perturbations, and a bifurcation occurs when this eigenvalue passes through zero. Solving $\lambda_1 = 0$ for ϵ defines the secondary bifurcation curve

$$\epsilon = \frac{1}{\sqrt{2}\pi}\sqrt{\frac{1-\gamma+\pi^2(1+\gamma)}{\pi^2+1}} \tag{5.12}$$

which approximates Γ_1.

The AIM-1 equations consist of higher order corrections to the AIM-0 system:

$$\frac{du_0}{dt} = -\sigma_0 u_0 + u_0 - u_0^3 - \frac{3}{2}u_0 u_1^2 + \mathcal{C}_0(u_0, u_1), \tag{5.13}$$

$$\frac{du_1}{dt} = -\sigma_1 u_1 + u_1 - \frac{3}{4}u_1^3 - 3u_0^2 u_1 + \mathcal{C}_1(u_0, u_1), \tag{5.14}$$

where

$$\mathcal{C}_0(u_0, u_1) = -\frac{27u_0^3 u_1^4}{8\sigma_2^2} - \left(\frac{3}{32\sigma_3^2} + \frac{9}{16\sigma_2\sigma_3}\right) u_0 u_1^6 + \frac{9u_0 u_1^4}{8\sigma_2}, \tag{5.15}$$

$$\mathcal{C}_1(u_0, u_1) = \frac{9u_1^3 u_0^2}{2\sigma_2} - \frac{27u_1^5 u_0^2}{8\sigma_2^2} - \frac{9u_1^5 u_0^2}{8\sigma_2\sigma_3} + \frac{27u_1^7 u_0^2}{64\sigma_3\sigma_2^2} + \frac{3u_1^5}{16\sigma_3} - \frac{3u_1^7}{32\sigma_3^2}. \tag{5.16}$$

The mode-one solutions are the nonzero real solutions of the equation

$$-\sigma_1 u_1 + u_1 - \frac{3}{4}u_1^3 + \frac{3u_1^5}{16\sigma_3} - \frac{3u_1^7}{32\sigma_3^2} = 0, \tag{5.17}$$

which is obtained by setting $u_0 = 0$ and $\frac{du_0}{dt} = 0$ in (5.14). Consider the polynomial

$$r(z) = 1 - \sigma_1 - \frac{3}{4}z + \frac{3z^2}{16\sigma_3} - \frac{3z^3}{32\sigma_3^2}. \tag{5.18}$$

which is obtained from (5.17) by factoring out the zero solution and letting $z = u_1^2$. Solutions to $r(z) = 0$ can be explicitly computed using the cubic formula. It is easy to check that r is a nonincreasing function and has at most one real root, z_1, which is nonnegative when $\sigma_1 \leq 1$ and negative when $\sigma_1 > 1$. The mode-one solutions are exactly $u_1 = \pm\sqrt{z_1}$ for $\sigma_1 \leq 1$.

The eigenvalues for the linearization of the AIM-1 system about a mode-one solution $(0, u_1)$ are

$$\lambda_1 = -\sigma_0 + 1 - \frac{3}{2}u_1^2 - \frac{3u_1^6}{32\sigma_3^2} - \frac{9u_1^6}{16\sigma_2\sigma_3} - \frac{9u_1^4}{8\sigma_2}, \tag{5.19}$$

$$\lambda_2 = -\sigma_1 + 1 - \frac{9u_1^2}{4} + \frac{15u_1^4}{16\sigma_3} - \frac{21u_1^6}{32\sigma_3^2}. \tag{5.20}$$

As in the case for AIM-0, a secondary bifurcation of the mode-one branch occurs as λ_1 passes through zero and hence the bifurcation curve is obtained by solving $\lambda_1 = 0$

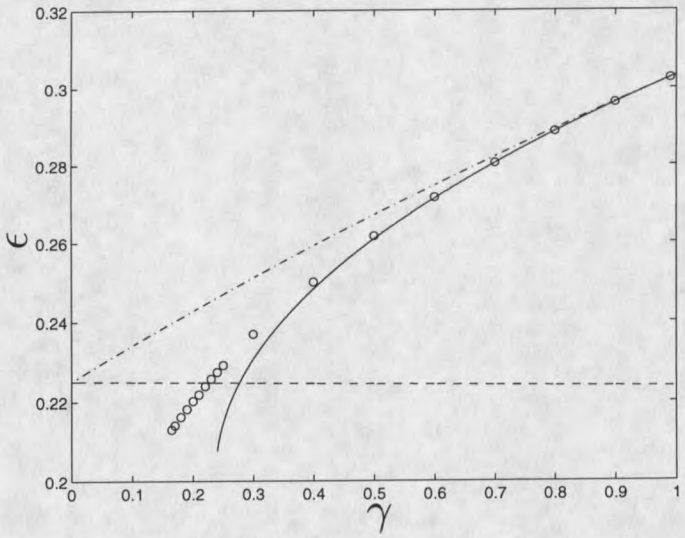


Figure 11: Mode-one secondary bifurcation points: AUTO (o), AIM-0 (-.-), AIM-1 (solid), Γ_s (- -).

for ϵ as a function of γ. To compute this curve, we substituted a mode-one solution of (5.17) into (5.19), and solved the equation $\lambda_1 = 0$ using Newton's method over a range of γ values.

A comparison of the approximate bifurcation curves obtained by these systems with the curve computed using the software package AUTO, is presented in Figure 11. Recall, Γ_s is the curve given by $\sigma_2 = 2$ which is the lower boundary for $\mathcal{U}$. From the figure we see that as $\gamma \to 1$, the bifurcation curves converge at the point $C_{0,1}$. We expect this to be the case since in a neighborhood of this point, the local analysis of Chapter 3 applies and the mode-one solutions are well approximated by $\pm\eta cos(\pi x)$ for some $\eta \ll 1$. Thus we expect the AIM-0 and AIM-1 systems to be rather accurate near this point. Proceeding away from the point in a direction of decreasing γ or ϵ these approximations become less accurate. We expect the nonlinear correction terms of AIM-1 system to provide an improvement over the AIM-0 system, and from the figure we see that it does in the sense that it is closer to the curve computed using AUTO.

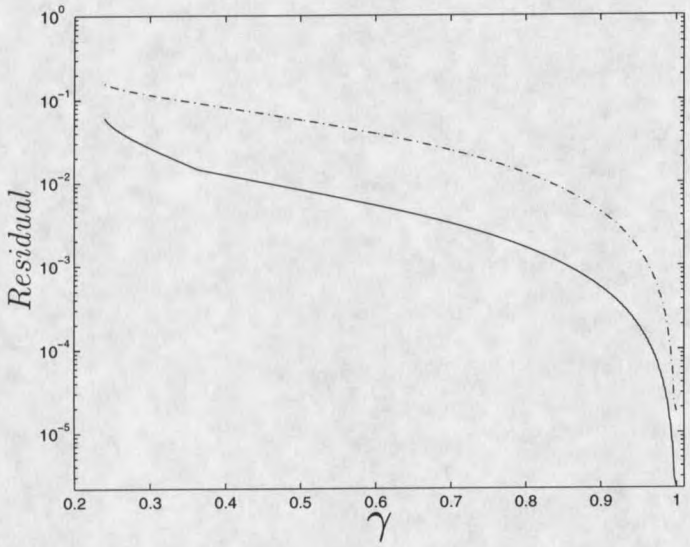


Figure 12: Mode-one residual errors at bifurcation points : AIM-0 (-.-), AIM-1 (-).

To obtain an additional quantitative comparison between AIM-0 and AIM-1 systems, we computed a residual error of the mode-one solutions at their bifurcation points (Figure 12). For an approximate solution u_a we defined the residual as

$$Residual = ||\epsilon^2 u_a'' + f(u_a) + \gamma B u_a||_\infty. \tag{5.21}$$

The results show that for γ sufficiently large, AIM-1 is consistently an order of magnitude more accurate than AIM-0 in this measure of error. An additional deficiency of AIM-0 can be seen in Figure 11. Secondary bifurcations occur in the case $\gamma = 0$, which we know do not exist for the Chafee-Infante equation. This demonstrates a limitation of this system and caution must be used when making any inferences from it.

Computing the Jacobian of the vector fields of the AIM-0 and AIM-1 systems at the zero solution yields in both cases

$$J = \begin{bmatrix} 1-\sigma_0 & 0 \\ 0 & 1-\sigma_1 \end{bmatrix}. \tag{5.22}$$

Thus, these systems capture the primary bifurcation curves M_0 and M_1 exactly. By a similar computation, we find that the curve Γ_0 of bifurcations from the constant solutions $m_0^{\pm} = \pm\sqrt{1-\gamma}$ is also exactly computed by these systems. From the analysis of Chapter 4, the AIM-0 error at equilibria is bounded by $\frac{C_F}{\Lambda}$, while for AIM-1 the error is bounded by $\frac{C_F C_{F'}}{\Lambda^2}$. Since Λ is strictly increasing in γ, $\frac{1}{\Lambda} \to 0$ as $\gamma \to \infty$. Thus in the parameter regime

$$\{(\gamma, \epsilon) \in \mathcal{U} : \gamma \gg 1\}$$

these systems should provide reasonable approximations of the nonlocal equation (2.7).

Figure 13 is a caricature of the bifurcation curves in $\mathcal{U}$ and Figure 14 shows a typical set of bifurcation diagrams for AIM-0 and AIM-1. The bifurcation structure for these systems is qualitatively similar to the results of the local analysis of Chapter 3. Consider the path **A** in $\mathcal{U}$ as depicted in Figure 13 obtained by fixing ϵ and allowing γ to vary. The zero solution is initially stable until the M_1 curve is crossed and the mode-one solutions appear. The constant solutions then appear, followed by mixed mode solutions which bifurcate from the constant solutions when Γ_0 is crossed. The mixed modes then coalesce with the mode-one solutions at the Γ_1 crossing. The result is an exchange of stability between the mode-one and constant solutions. Using AUTO we were able to duplicate these results and a comparison (Figures 15 and 16) indicates that the AIM systems do a reasonable job of qualitatively capturing the secondary bifurcations.

Figure 17 shows the four mixed mode solutions computed by AUTO on the secondary bifurcation curves of Figure 16. To fix our notation for the remainder of this thesis we will denote the mixed mode solutions as $m_s^{(k)}$, $k = 1, \ldots, 4$, where the superscript indicates the quadrant of the $u_0 - u_1$ plane containing the corresponding AIM approximation.

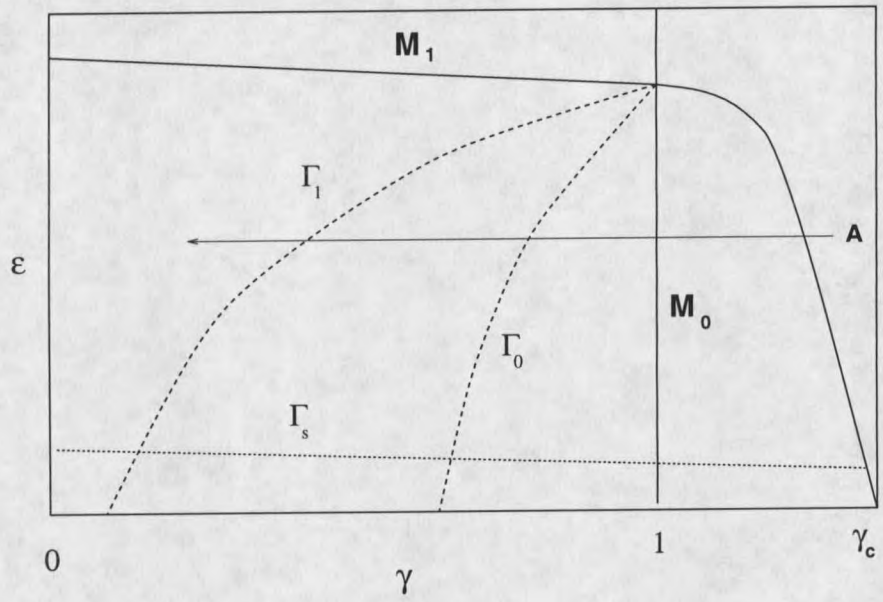


Figure 13: Bifurcation curves in the region $\mathcal{U}$.

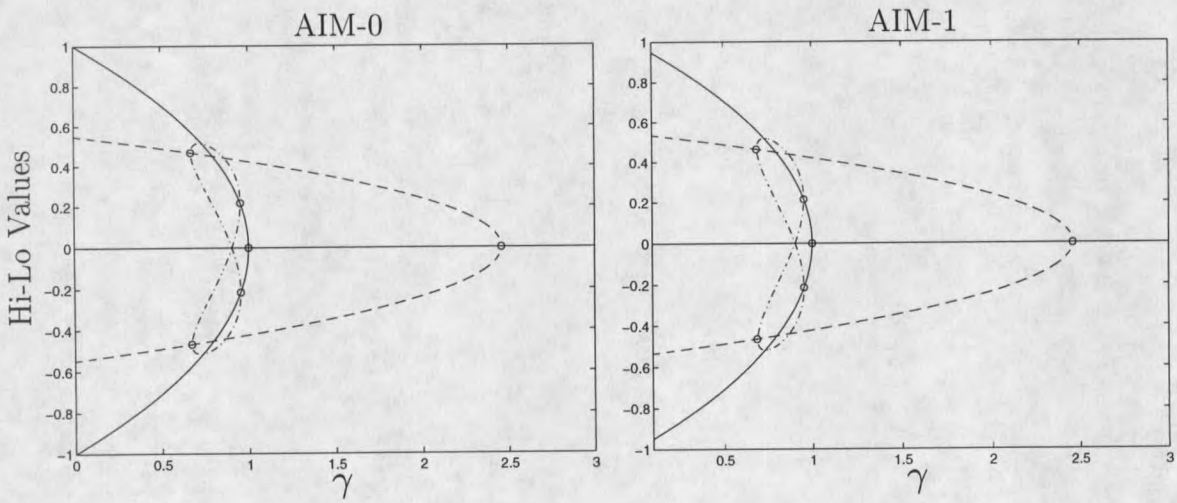


Figure 14: γ-Bifurcation diagrams on path **A** for $\epsilon = 0.28$: constant solutions (solid), mode-one (- -), mixed modes (-.-).

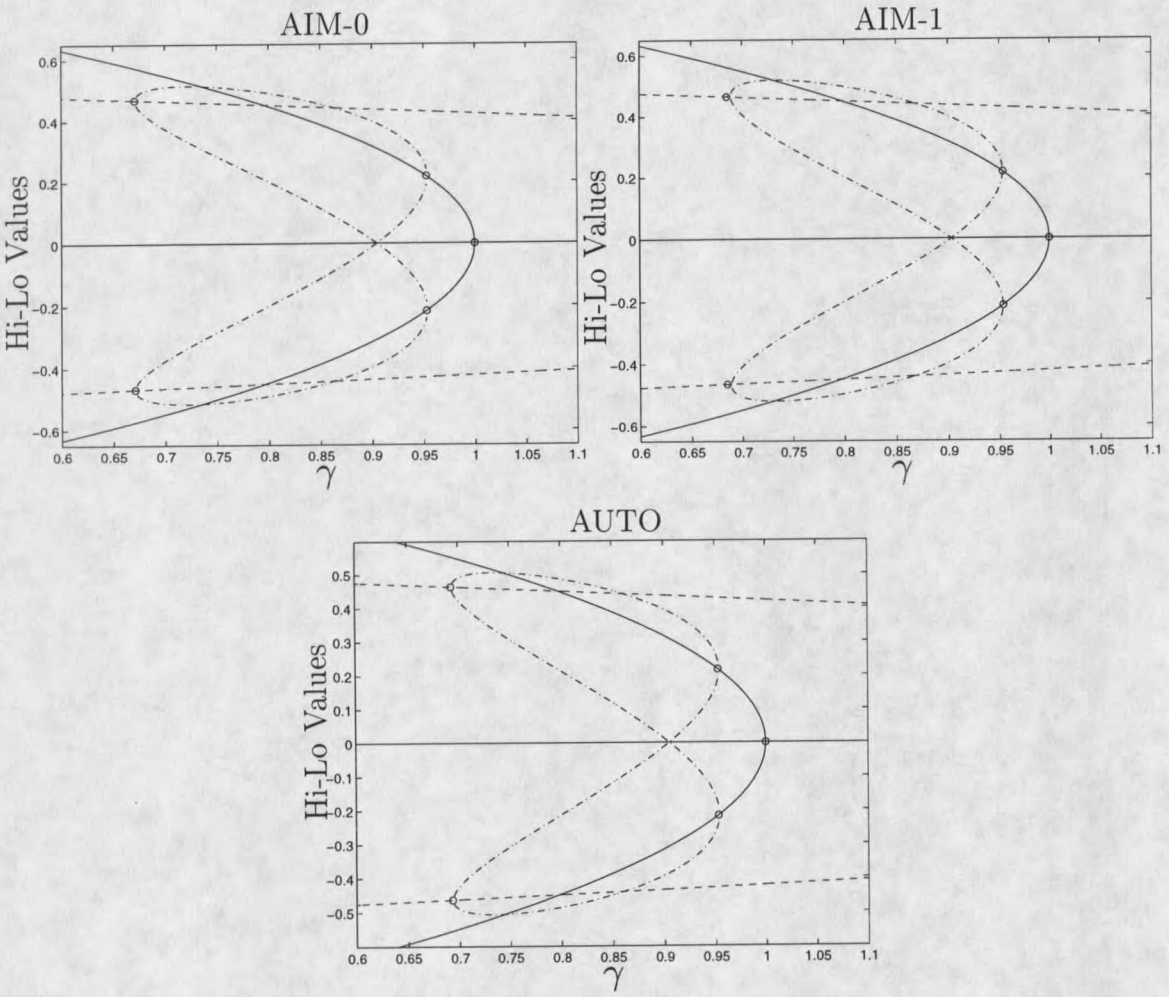


Figure 15: γ-Bifurcation diagrams for $\epsilon = 0.28$: constant solutions (solid), mode-one (- -), mixed modes (-.-).

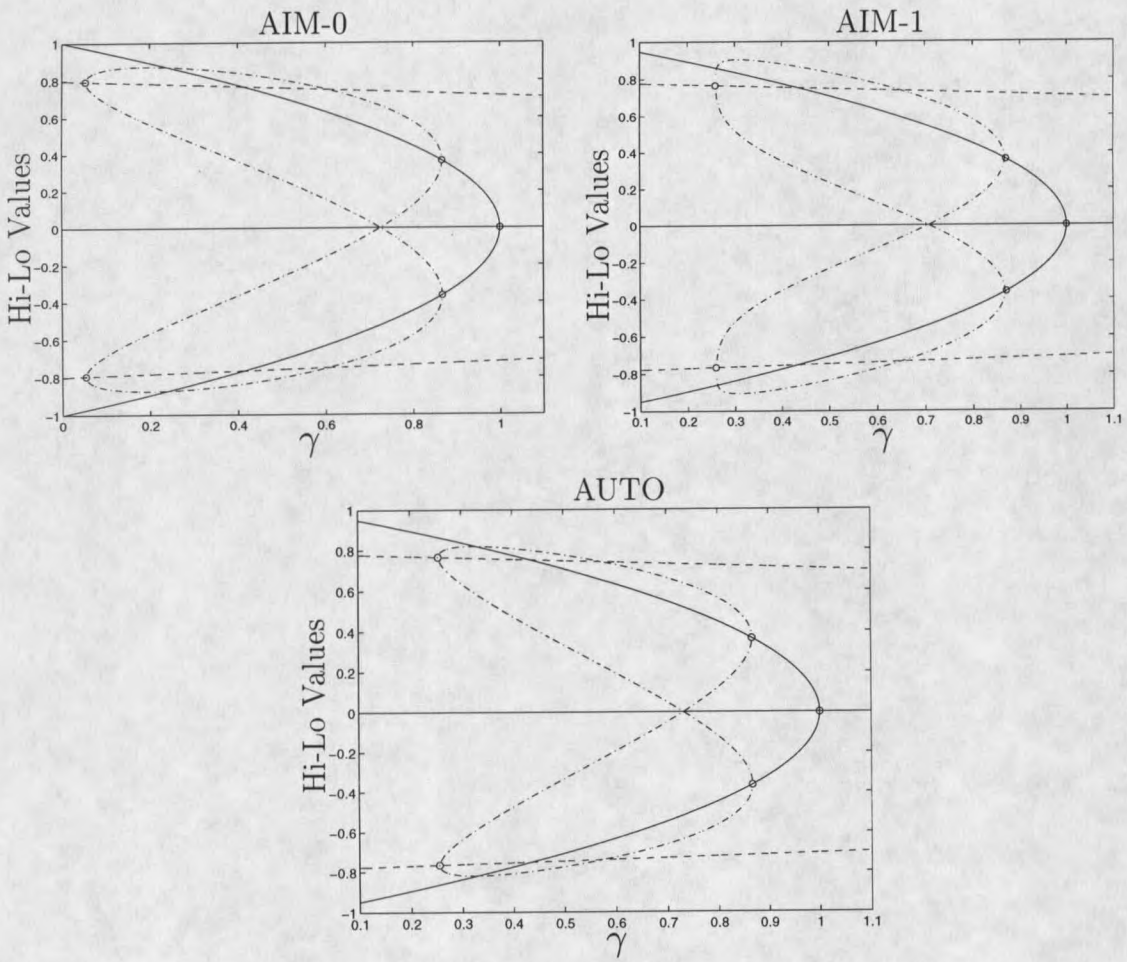


Figure 16: γ-Bifurcation diagrams for $\epsilon = 0.23$: constant solutions (solid), mode-one (- -), mixed modes (-.-).

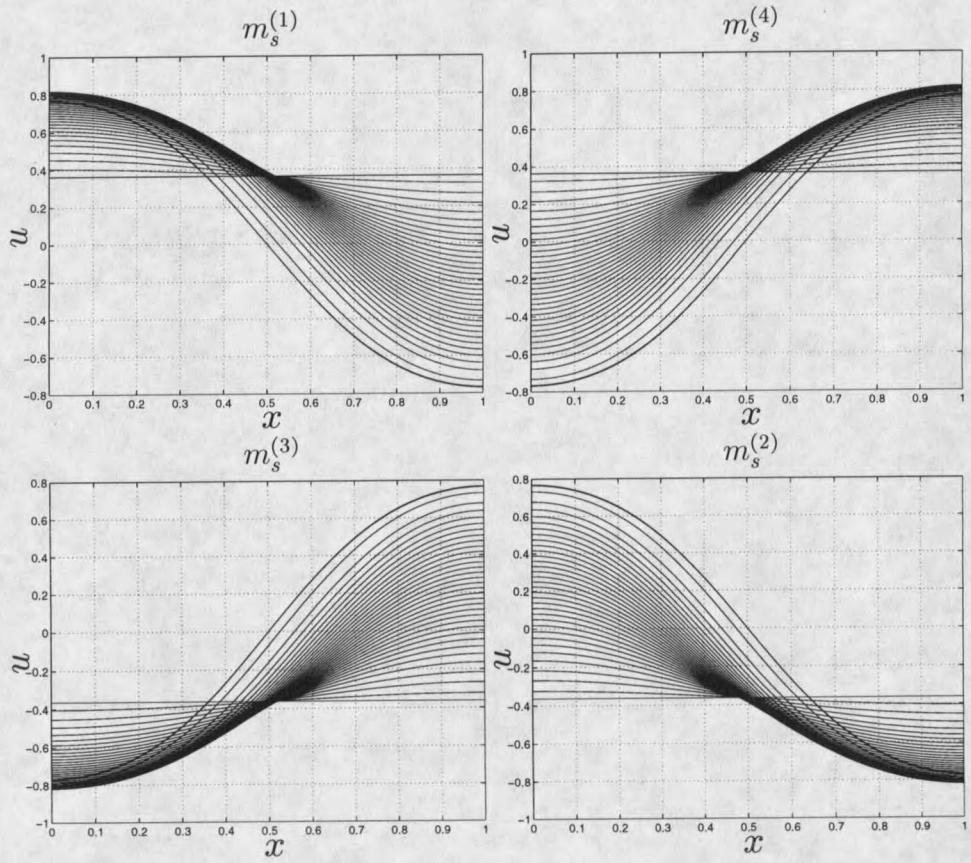


Figure 17: Mixed mode solutions computed by AUTO: $\epsilon = 0.23$, $0.2 \leq \gamma \leq 0.87$.

The results we've obtained here seem to indicate that the bifurcation picture we see from the local analysis, is in fact a global phenomena in the region $\mathcal{U}$.

Approximation of the Connecting Orbits

The location of equilibria is only one step in forming a description of the attractor for the evolution equation (2.7). Since equation (2.7) generates a semigroup which is a gradient system, the attractor consists of the equilibria and their unstable manifolds. When the equilibria are hyperbolic, that is away from any bifurcations, they are isolated and their unstable manifolds form connecting orbits. In this section, we will locate and approximate the orbits which form the connections between the

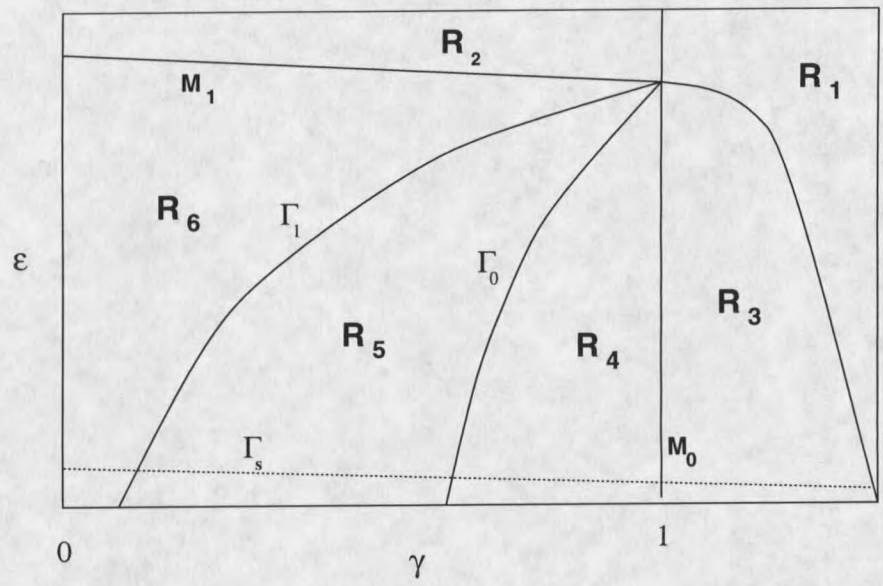


Figure 18: Regions in parameter space.

solutions found in the previous results. The region $\mathcal{U}$ can be further divided into subregions by the bifurcation curves as depicted in Figure 18. In each of these subregions the attractor is expected to be qualitatively distinct from the adjacent regions.

We will first search for the heteroclinic connections using the two-dimensional approximate inertial manifolds. The inertial forms are planar systems for which we can easily analyze the dynamics. Once we find these connections, we will then numerically verify that similar connections exists for the evolution equation (2.1) using a numerical shooting method based on a standard finite difference scheme.

Dynamics of the Inertial Forms

The dynamics of the inertial forms is easy to analyze in the phase-plane and in Figure 19 we have representative depiction of the direction field, equilibria and connecting orbits for AIM-1 in each of the subregions. These results were obtained using the Matlab routine *pplane.m* [17]. The qualitative behavior for the AIM-0 system is identical. In the region R_1, the zero solution is the global attractor for the system.

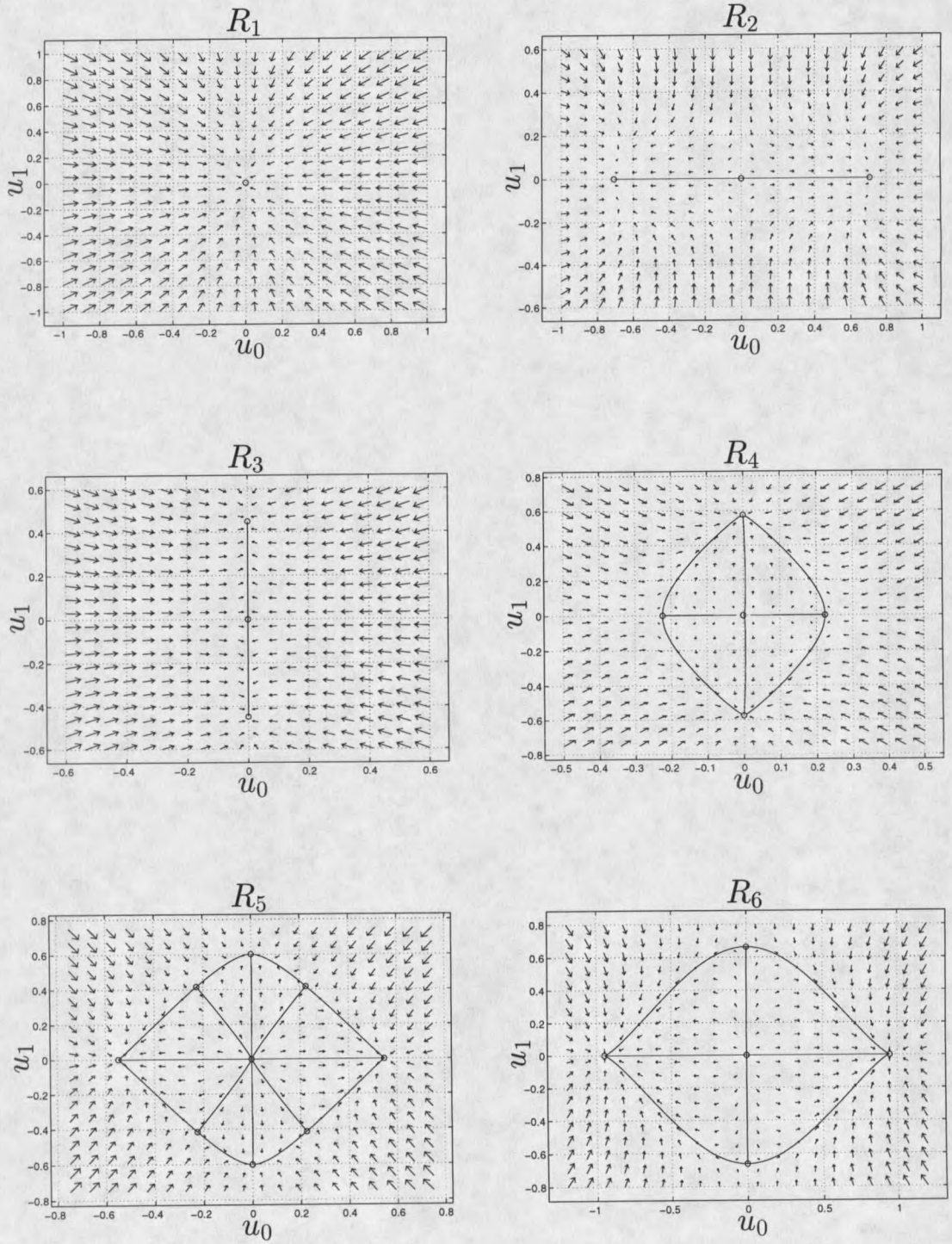


Figure 19: Attractors for AIM-1.

Passing from R_1 to R_2 zero becomes unstable as the constant mode solutions bifurcate from zero. The bifurcating constant solutions are stable and there is a heteroclinic connection from zero to each of these solutions.

Passing from R_1 to R_3 the mode-one solutions bifurcate from zero and are stable in all of R_3. The one-dimensional unstable manifold of the zero solution forms a heteroclinic connection to these solutions. In R_4 the equilibria consist of zero, the nonzero constant solutions and the mode-one solutions. In this region, the constant solutions are unstable and are connected to the mode-one solutions. Passing through R_5 to R_6 the nature of the secondary bifurcations becomes very apparent. The mixed mode solutions, which exist in R_5, block the heteroclinic connection between the constant mode and mode-one solutions. In passing from R_4 to R_6 through R_5 the end result is an exchange of stability between the nonzero constant and mode-one solutions by a reversal of the heteroclinic connections between them. Figure 20 shows the attractor in R_5 near the secondary bifurcations and an intermediate point.

In R_6 the only stable solutions are the nonzero constant solutions and the attractor is qualitatively similar to the attractor for the Chafee-Infante system.

In the following, we will provide numerical evidence that the attractor for (2.7), contains at least the structure we have found in the inertial forms.

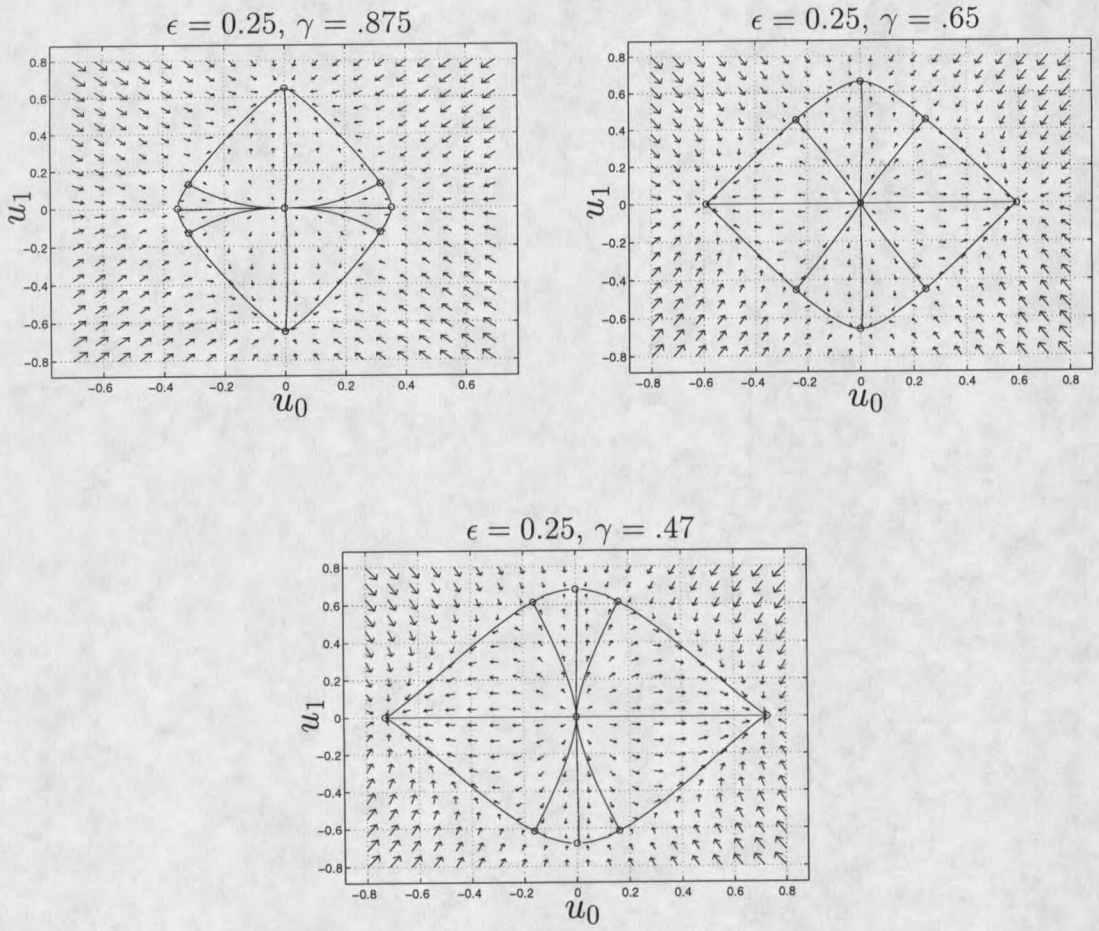


Figure 20: Attractors for AIM-1 passing through R_5.

Numerical Computation of Connecting Orbits

Consider two equilibria u_- and u_+ of (2.7). A heteroclinic connection from u_- to u_+ exists if there is a solution to the problem

$$u_t = -Au + f(u), \tag{5.23}$$

$$u(-\infty) = u_-, \quad u(+\infty) = u_+. \tag{5.24}$$

To approximate a connection we consider the problem on a finite but large time interval $[-\frac{T}{2}, \frac{T}{2}]$,

$$u_t = -Au + f(u), \tag{5.25}$$

$$u\left(-\frac{T}{2}\right) = u_-, \quad u\left(\frac{T}{2}\right) = u_+. \tag{5.26}$$

This can be considered as a functional boundary value problem in t and methods have been developed [2] for numerically solving this problem in general. For our case, since the unstable manifolds of the equilibria have dimension at most two, and we suspect the connections to be one-dimensional, we will make use of a much simpler shooting method. Rescaling time we have

$$u_t = T(-Au + f(u)), \tag{5.27}$$

$$u(0) = u_-, \quad u(1) = u_+. \tag{5.28}$$

Now suppose $W^u_{loc}(u_-) = span\{v_1, v_2\}$. For initial data we will use a small perturbation from u_- on $W^u_{loc}(u_-)$

$$u(0) = u_- + \eta[cos(\theta)v_1 + sin(\theta)v_2], \quad \eta \ll 1. \tag{5.29}$$

Defining

$$\mathcal{J}(\theta) = \frac{1}{2}||u(\theta, 1) - u_+||^2_0, \tag{5.30}$$

we wish to find θ for which $\mathcal{J}(\theta) = 0$. To do this we will use Newton iterations

$$\theta_{n+1} = \theta_n - \frac{\mathcal{J}(\theta_n)}{\mathcal{J}'(\theta_n)}, \tag{5.31}$$

where the derivative of $\mathcal{J}$ is given by

$$\mathcal{J}'(\theta) = \int_0^1 (u(\theta, 1) - u_+) y(1) dx \tag{5.32}$$

with y being the solution to the linearized problem

$$y_t = T(-Ay + f'(u(\theta, t))y), \tag{5.33}$$

$$y(0) = \eta[-sin(\theta)v_1 + cos(\theta)v_2]. \tag{5.34}$$

In the cases where $W^u_{loc}(u_-) = span\{v_1\}$ is one-dimensional, we can approximate the connection by simply solving the initial value problem with $u(0) = u_- + \eta v_1$, $\eta << 1$, until $\mathcal{J}(0)$ is sufficiently small.

To implement this method, we spatially discretize equations (5.27), (5.28), (5.33) and (5.34) using a standard finite difference scheme. To discretize the operator A, let M be the standard centered difference approximation of the second derivative with homogeneous Neumann boundary conditions and I the identity matrix. Then we approximate A by

$$\tilde{A} = \epsilon^2 M + \gamma(M - I)^{-1}. \tag{5.35}$$

Now letting $\vec{U} = (U_1, U_2, \ldots, U_m)^T$, and $\vec{Y} = (Y_1, Y_2, \ldots, Y_m)^T$ we have

$$\frac{d\vec{U}}{dt} = T(\tilde{A}\vec{U} + \vec{F}(\vec{U})), \tag{5.36}$$

$$\vec{U}(0) = \vec{U}_- + \eta[cos(\theta)\vec{V}_1 + sin(\theta)\vec{V}_2], \tag{5.37}$$

$$\frac{d\vec{Y}}{dt} = T(\tilde{A}\vec{Y} + D\vec{F}(\vec{U})\vec{Y}), \tag{5.38}$$

$$\vec{Y}(0) = \eta[-sin(\theta)\vec{V}_1 + cos(\theta)\vec{V}_2], \tag{5.39}$$

where

$$\vec{F}(\vec{U}) = (U_1 - U_1^3, U_2 - U_2^3, \ldots, U_m - U_m^3)^T, \tag{5.40}$$

$D\vec{F}(\vec{U})$ is the Jacobian matrix of $\vec{F}(\vec{U})$, and $\vec{U}_-$, $\vec{U}_+$, $\vec{V}_1$ and $\vec{V}_2$ are the discrete approximations of the equilibria and the unstable eigenfunctions. The Newton iterations are then performed using the discrete functions

$$\hat{\mathcal{J}}(\theta) = \frac{1}{2}(\vec{U}(1,\theta) - \vec{U}_+)^T(\vec{U}(1,\theta) - \vec{U}_+), \tag{5.41}$$

$$\hat{\mathcal{J}}'(\theta) = (\vec{U}(1,\theta) - \vec{U}_+)^T\vec{Y}(1) \tag{5.42}$$

until the value of $\hat{\mathcal{J}}(\theta)$ is below a prescribed tolerance.

In our computations we used a uniform spatial grid of 100 points. The discrete equilibria $\vec{U}_-$ and $\vec{U}_+$ were found by solving the steady state equation

$$\tilde{A}\vec{U} + \vec{F}(\vec{U}) = 0, \tag{5.43}$$

via Newton's method using the the AIM-0 solutions as an initial guess. Newton iterations were performed until $||\tilde{A}\vec{U} + \vec{F}(\vec{U})||_\infty \leq 10^{-10}$. When the eigenvectors corresponding to the local unstable manifolds of U_- could not be found in closed form, they were numerically computed from the Jacobian matrix $D\vec{F}(\vec{U}_-)$ using the Matlab routine *eig.m*. The semi-discrete system was numerically integrated using the Matlab routine *ode15s.m* which is a variable order method for stiff systems. In all cases the perturbation amplitude was take to be $\eta = 0.001$ and the equations were integrated until $\hat{\mathcal{J}} < 10^{-5}$.

The evolution equation possess a symmetry, knowledge of which reduces the amount computation we will need to do. Define

$$H_{odd} = span\{cos((2n+1)\pi x), n = 0, 1, \ldots\}$$

and

$$H_{even} = span\{cos(2n\pi x), n = 0, 1, \ldots\}.$$

If u is a solution of (2.7), then $u = u_o + u_e$, where $u_o \in H_{odd}$, and $u_e \in H_{even}$ solve

$$\frac{du_o}{dt} = -Au_0 + f(u_o) - 3u_o u_e^2, \tag{5.44}$$

$$\frac{du_e}{dt} = -Au_e + f(u_e) - 3u_e u_o^2. \tag{5.45}$$

But $f : H_{odd} \to H_{odd}$, $f : H_{even} \to H_{even}$, $u_o u_e^2 \in H_{odd}$, and $u_e u_o^2 \in H_{even}$. Therefore, these spaces are invariant for (2.7). Moreover, if $u = u_e + u_o$ is a solution then so are $-u$, $-u_e + u_o$, and $u_e - u_o$. Because of this symmetry we need only verify the connections for approximate inertial forms which are in the closed first quadrant of the plane.

Regions R_1 and R_2

In these two regions $\sigma_n > 0$ for $n > 0$ and no non-constant bifurcations from the zero solution occur. By Lemma 4.4, we know that when $\sigma_1 > 2$ the large time dynamics are determined by the differential equation

$$\frac{du}{dt} = -\gamma u + f(u). \tag{5.46}$$

Moreover, the attractor for (5.46) is the attractor for (2.7). This result, however, does not hold in all of regions R_1 and R_2. To see that the zero solution is the global attractor in R_1, let u be a solution. Multiplying (2.7) by u and integrating we have

$$\begin{aligned} \frac{1}{2}\frac{d}{dt}||u||_0^2 &= -(Au, u) + (f(u), u)_0, & (5.47)\\ &= -||u||_1^2 + ||u||_0^2 - \int_0^1 u^4 dx, & (5.48)\\ &\leq (1 - \sigma_p)||u||_0^2. & (5.49) \end{aligned}$$

Since $\sigma_p > 1$, $||u||_0^2 \to 0$ at $t \to \infty$.

In R_2 the attractor for (5.46) is as depicted in Figure 21. It is not clear that this is the global attractor for (2.7). The invariant manifold of constant solutions is, however, locally normally attracting. To see this, let u be a solution of (5.46). Consider the linear variational equation of (2.7) with respect to a perturbation v,

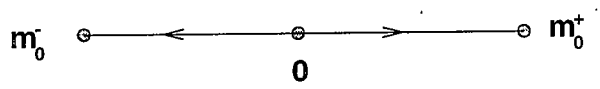


Figure 21: Attractor for R_2.

with $\int_0^1 v dx = 0$, which is given by

$$v_t = -Av + f'(u(t))v. \tag{5.50}$$

Multiplying this equation by v and integrating we have

$$\begin{aligned} \frac{1}{2}\frac{d}{dt}||v||_0^2 &= -(Av, v)_0 + f'(u(t))||v||_0^2, & (5.51)\\ &= -||v||_1^2 + ||v||_0^2 - 3(u(t))^2||v||_0^2, & (5.52)\\ &\leq (1-\sigma_1)||v||_0^2 - 3(u(t))^2||v||_0^2. & (5.53) \end{aligned}$$

We see that since $\sigma_1 > 1$, v decays to zero in $L^2(0,1)$. So the attractor for (5.46) is at least a local attractor for the evolution equation. Since the space of constant functions is invariant for (2.7), these connections exist in all of parameter space where $\gamma < 1$.

Region R_3

In region R_3 the mode-one solutions have bifurcated from zero and the zero solution has a one-dimensional unstable manifold with $W^u_{loc}(0) = span\{cos(\pi x)\}$. We numerically computed the connection from zero to the mode-one solution m_1^+ and the results are presented in Figure 22. By the invariance of H_{odd} we have $W^u(0) \subset H_{odd}$. No additional bifurcations from zero occur in this region. Moreover, the mode-one solutions seems to remain stable. Figure 23 depicts the equilibria and connections in R_3 for which we have numerical support. It is not clear that this is the global attractor but we can conclude that the attractor for (2.7) is contained in H_{even}. To

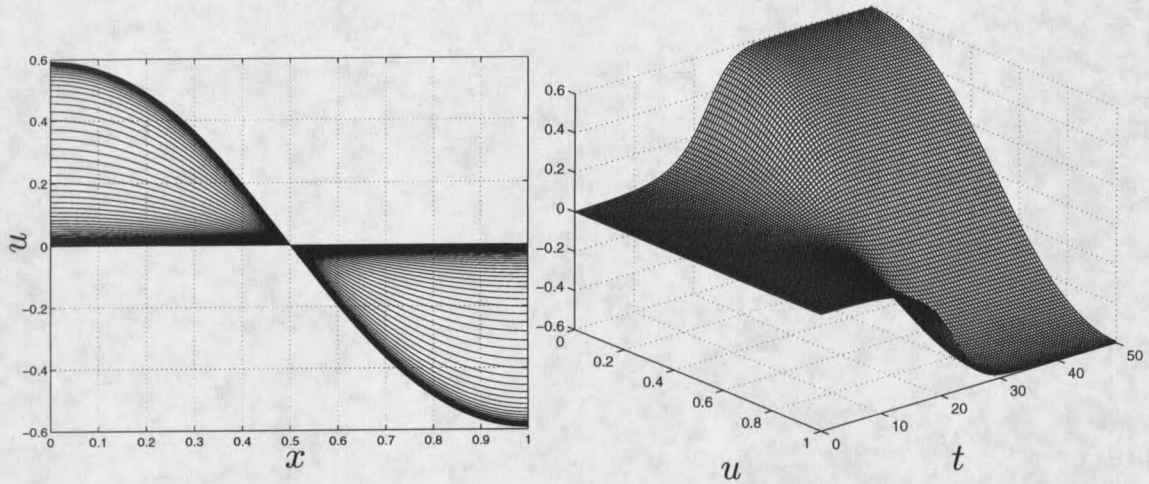


Figure 22: R_3 Connection from zero to m_1^+ : $\alpha = 1.25$, $\epsilon = 0.25$.

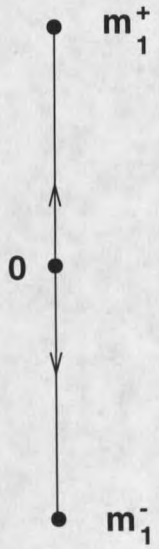


Figure 23: Equilibria and connections for R_3.

see this, consider the equation (5.45) for the even solution components. Multiplying this equation by u_e and integrating we have

$$\frac{1}{2}\frac{d}{dt}||u_e||_0^2 = -(Au_e+, u_e)_0 + (f(u_e), u_e)_0 - (3u_e^2, u_o^2)_0, \tag{5.54}$$

$$= -||u_e||_1^2 + ||u_e||_0^2 - (u_e^2, u_e^2)_0 - (3u_e^2, u_o^2)_0, \tag{5.55}$$

$$\leq (1-\sigma_e)||u_e||_0^2 - (u_e^2, u_e^2)_0 - (3u_e^2, u_o^2)_0. \tag{5.56}$$

where σ_e is the principle eigenvalue of A restricted to H_{even}. Since $\sigma_e > 1$, we see that $||u_e||_0^2$ decays to zero. Using an argument similar to that used for R_2 one can show that the manifold connecting zero to m_1^+ is locally normally attracting.

Region R_4

In region R_4 the mode-one solutions appear to be stable, the zero solution is unstable with $W^u_{loc}(0) = span\{1, cos(\pi x)\}$, and the constant solutions are unstable with $W^u_{loc}(m_0^{\pm}) = span\{cos(\pi x)\}$. Figure 24 shows the numerical computation of the connection from zero to the mode-one solution, m_1^+. In Figure 25 we have the connection from the constant solution, $m_0^+ = \sqrt{1-\gamma}$, to m_1^+. The equilibria and connections for this region appear to be as depicted in Figure 26.

Region R_5

This region occurs after the secondary bifurcation from the constant solutions but prior to the secondary bifurcation of the mode-one branch. The bifurcation from the constant solutions yields four solutions $m_s^{(k)}$,$k = 1, \ldots, 4$, each having a one-dimensional unstable manifold. In this region, the mode-one solutions seem to be stable. The connection from zero to m_1^+ was computed and the results appear in Figure 27. The mixed mode solution $m_s^{(1)}$, and the eigenfunction corresponding to $W^u_{loc}(m_s^{(1)})$, was computed by the method we previously described. These solutions

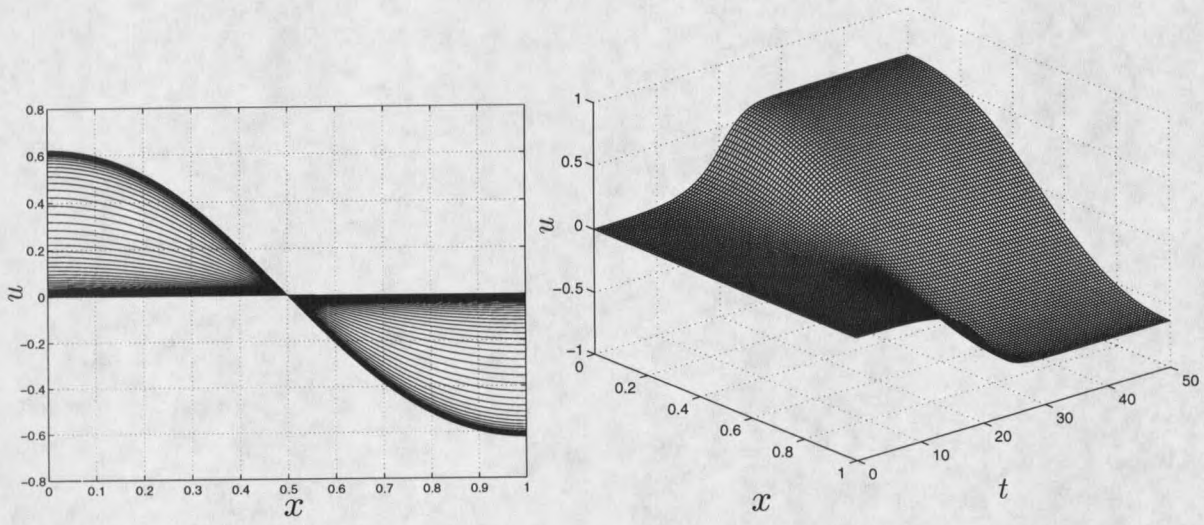


Figure 24: R_4 connection from zero to m_1^+ : $\alpha = 0.95$, $\epsilon = 0.25$.

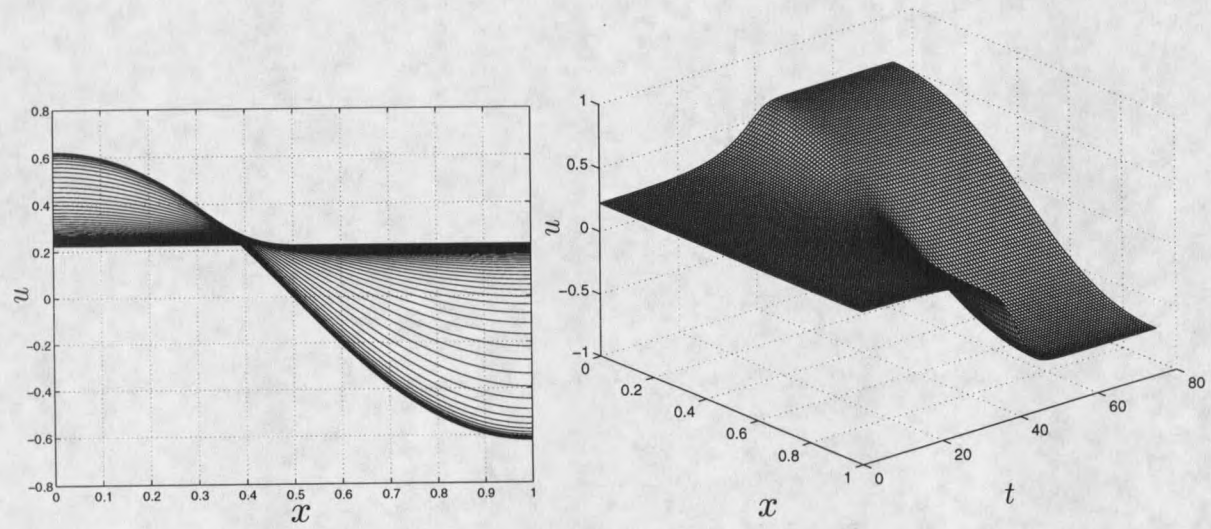


Figure 25: R_4 connection from m_0^+ to m_1^+ : $\alpha = 0.95$, $\epsilon = 0.25$.

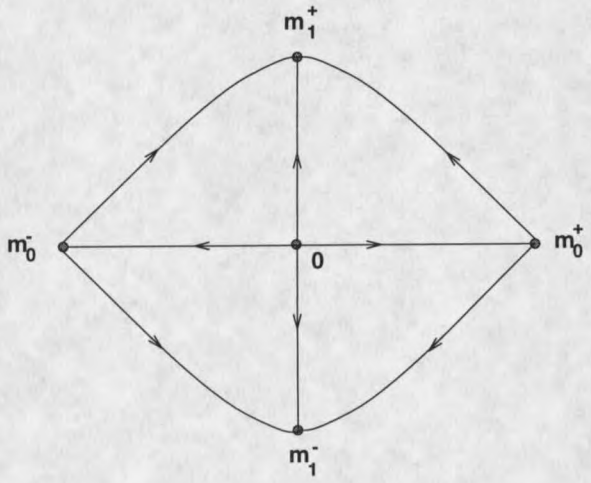


Figure 26: Equilibria and connections for R_4.

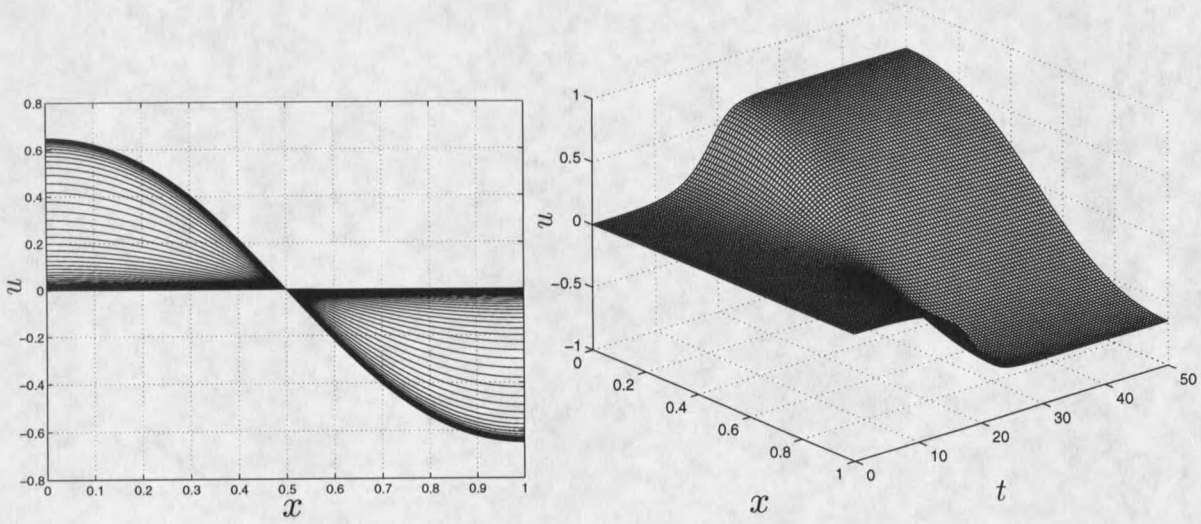


Figure 27: R_5 connection from zero to m_1^+ : $\alpha = 0.65$, $\epsilon = 0.25$.

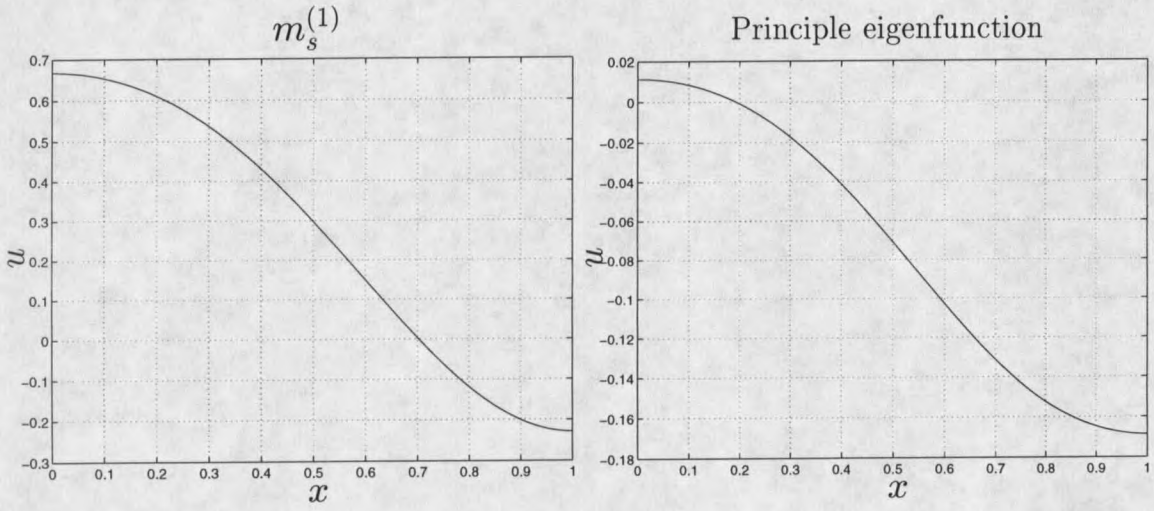


Figure 28: Mixed mode solution $m_s^{(1)}$ and its principle eigenfunction: $\alpha = .65$, $\epsilon = 0.25$.

appear in Figure 28. Using these results we computed the connections from $m_s^{(1)}$ to the mode-one solution m_1^+ and the constant solution m_0^+, which appear in Figures 29 and 30, respectively.

To compute the connection from zero to $m_s^{(1)}$ we used the shooting method with Newton iterations. This required a significant amount of trial and refinement to obtain satisfactory results. For parameter values near the secondary bifurcation curves Γ_0 and Γ_1 we were unable to satisfactorily compute the connections. In these cases, the connection seems to be nearly tangent to the connections from zero to the stable solutions which we can see from Figure 20. For values away from the bifurcations the method works rather well. Using a course grid of 25 points and an initial angle approximated from the AIM-1 connection, we performed computations and adjusted the final time, T, until we seemed to obtain convergence of the Newton iterations. Using the computed value of θ, and the time T, we then computed the connection for the system on the 100 point grid. The final connection is shown in Figure 31.

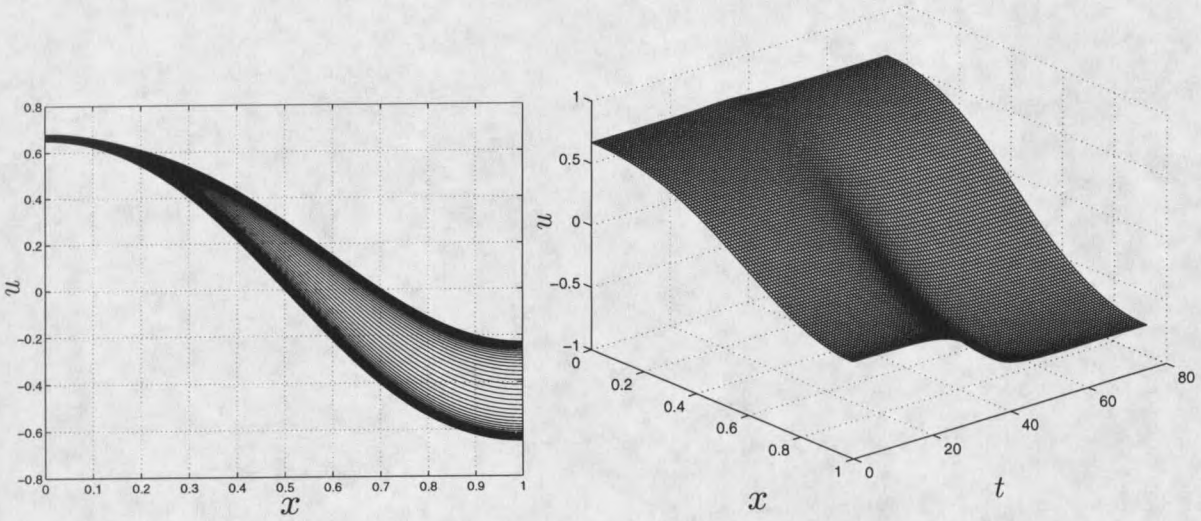


Figure 29: Connection from $m_s^{(1)}$ to m_1^+ : $\alpha = 0.65$, $\epsilon = 0.25$.

This connection was computed with $T = 62$, $\eta = 0.001$, $\theta \approx 1.2346$, and the final value of $\hat{\mathcal{J}}(\theta) = 7.667. \times 10^{-7}$. To compute the connection from zero to $m_s^{(1)}$ we used the shooting method with Newton iterations. This required a significant amount of trial and refinement to obtain satisfactory results. For parameter values near the secondary bifurcation curves Γ_0 and Γ_1 we were unable to satisfactorily compute the connections. In these cases, the connection seems to be nearly tangent to the connections from zero to the stable solutions which we can see from Figure 20. For values away from the bifurcations the method works rather well. Using a course grid of 25 points and an initial angle approximated from the AIM-1 connection, we performed computations and adjusted the final time, T, until we seemed to obtain convergence of the Newton iterations. Using the computed value of θ, and the time T, we then computed the connection for the system on the 100 point grid. The final connection is shown in Figure 31. This connection was computed with $T = 62$, $\eta = 0.001$, $\theta \approx 1.2346$, and the final value of $\hat{\mathcal{J}}(\theta) = 7.667. \times 10^{-7}$.

These results provide numerical justification for the connections as depicted

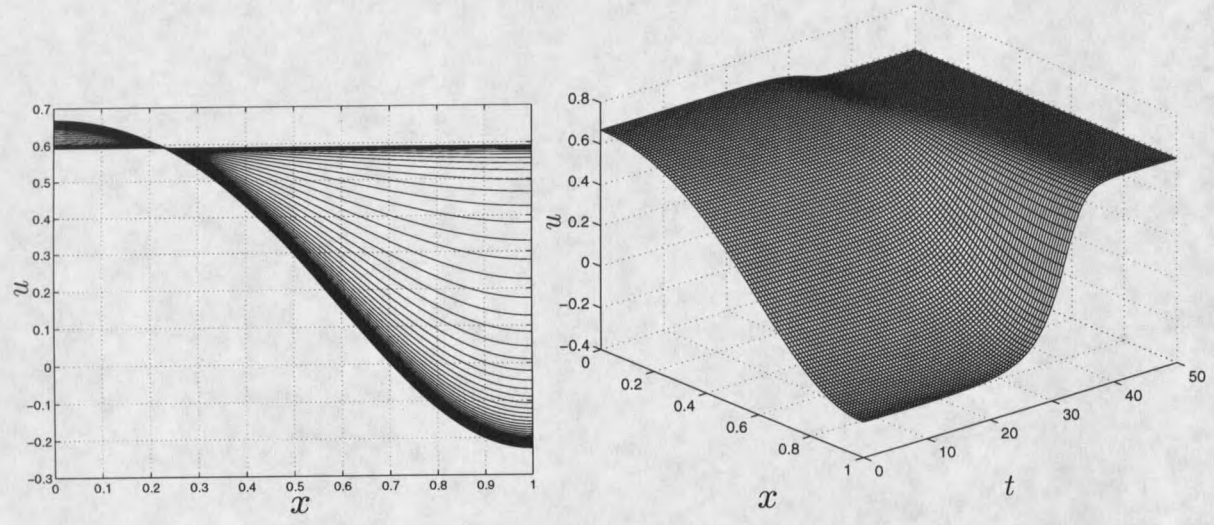


Figure 30: Connection from $m_s^{(1)}$ to m_0^+ : $\alpha = 0.65$, $\epsilon = 0.25$.

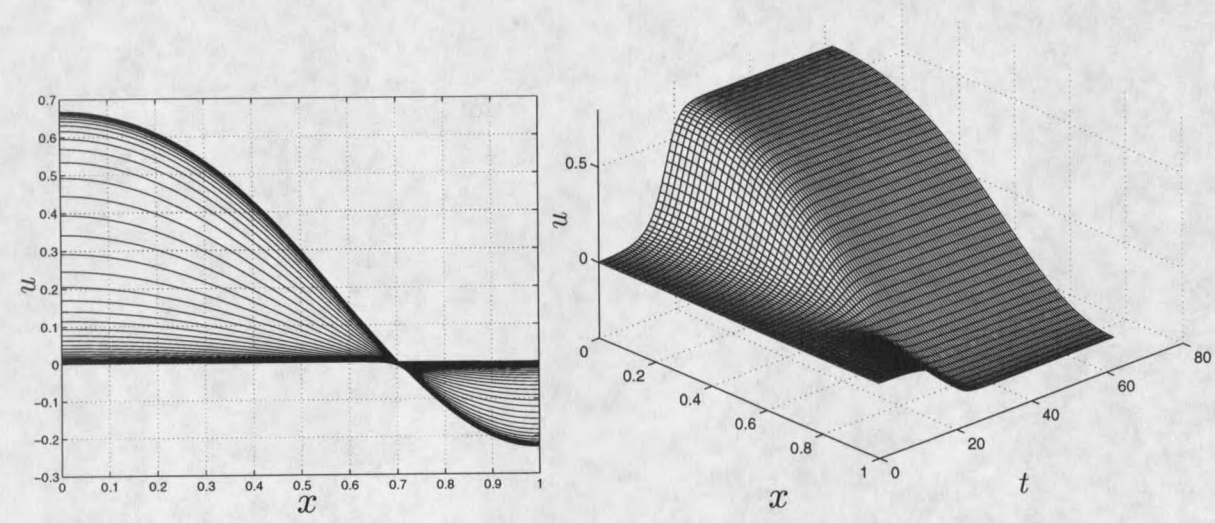


Figure 31: Connection from zero to $m_s^{(1)}$: $\alpha = 0.65$, $\epsilon = 0.25$.

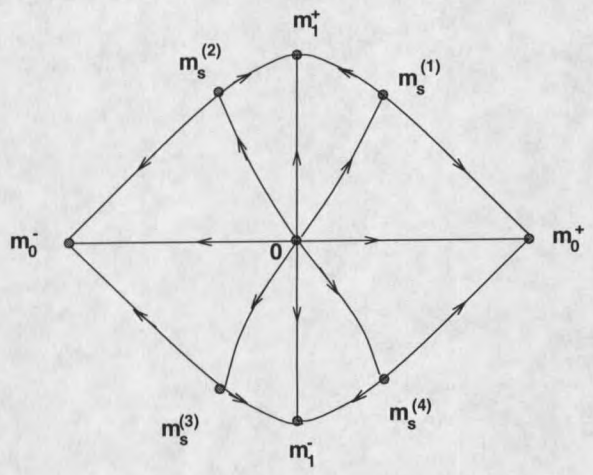


Figure 32: Equilibria and connections for R_5.

in Figure 32. We need to eliminate connections other than those shown. By the definition of the Lyapunov function V we know that the unstable manifold of an equilibria ϕ forms a connection to another equilibria ψ only if $V(\phi) > V(\psi)$. From the properties of the Lyapunov function V we know

$$V(m_0^+) = V(m_0^-), \tag{5.57}$$

$$V(m_1^+) = V(m_1^-), \tag{5.58}$$

$$V(m_s^{(j)}) = V(m_s^{(k)}), \quad j,k = 1,\ldots 4. \tag{5.59}$$

The only possible connections not shown in the figure would be from the solutions $m_s^{(k)}$ to $m_0^{\pm}$ and $m_1^{\pm}$. Such a connection might exist for example from $m_s^{(1)}$ to m_0^- and m_1^-. However since $dim W^u(m_s^{(1)}) = 1$ and we have established the connection to m_1^+ and m_0^+ there can be no others. Similar results hold for the remaining solutions. Therefore, for the known solutions the connections are as depicted in the figure.

Region R_6

In this region the attractor seems to contain the structure of the attractor for the Chafee-Infante problem which is depicted in Figure 33.

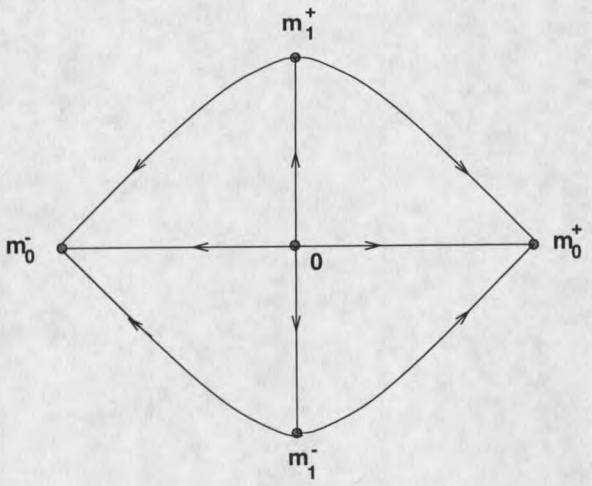


Figure 33: Equilibria and connections for R_6.

In summary, we have presented evidence for the subsets of the attractor which qualitatively appear as in Figure 34.

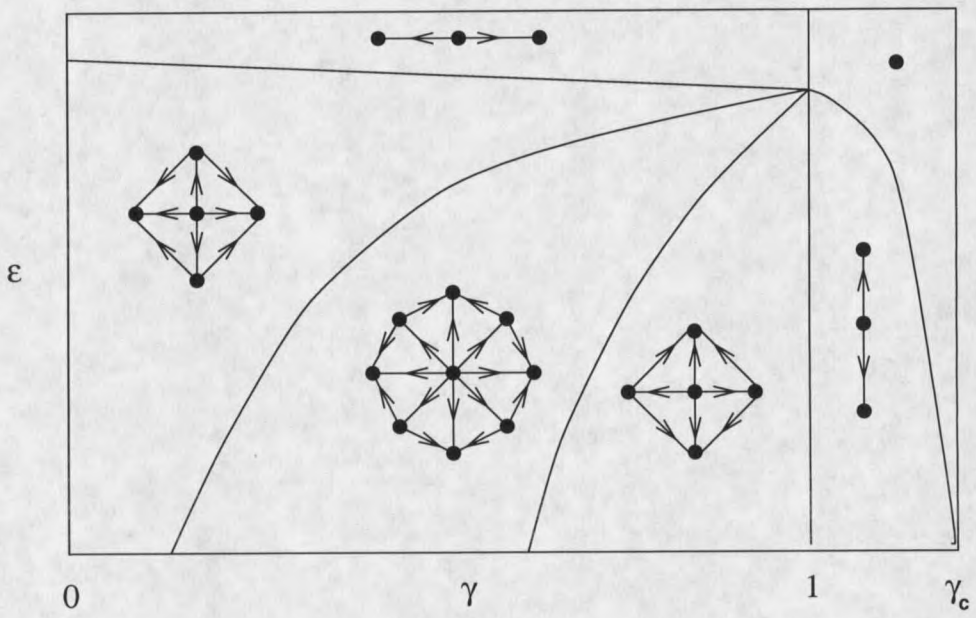


Figure 34: Summary of equilibria and connections in $\mathcal{U}$.

CHAPTER 6

CONCLUDING REMARKS

In this thesis, we have analyzed the nonlocally perturbed reaction-diffusion equation (1.1) and have provided evidence for the qualitative structure of a limited portion of the global attractor. Also, it was shown the addition of a nonlocal perturbation to the Chafee-Infante problem (1.4) can significantly alter the dynamics. For (1.4), all equilibria have a single dominant mode and there are no secondary bifurcations. The addition of nonlocal feedback allows a mixing of the dominant modes and such mixed mode solutions appear via secondary bifurcations. These secondary bifurcations can result in an exchange of stability between two solutions by the reversal of an orbit which connects them. This phenomenon is an interesting departure from the dynamics of (1.4). Unlike the Chafee-Infante problem, the number of internal transition layers of an equilibrium for (1.1) does not determine its Morse index and the direction of flow on connecting orbits is not exclusively in the direction which reduces the number of transition layers. Flow can proceed in a direction as to create a transition layer. Also, the spatially heterogeneous solutions can be stable, which is never the case for (1.4).

The global bifurcation diagram for (1.1) is clearly more complicated than that of the Chafee-Infante problem. From the bifurcation curves of Figure 4, and knowledge of the dynamics of the small γ case, the following conjecture seems probable:

Conjecture 6.1 *Let u be an n-mode equilibrium solution of (1.1), with $\gamma \ll 1$ sufficiently small that $dim W^u(u) = n$. Then there exists a sequence $\gamma_1 < \gamma_2 < \ldots < \gamma_n$ depending on ϵ so that for ϵ fixed each (γ_k, ϵ) , $k = 1, \ldots, n$,is a bifurcation point.*

Moreover, in passing through the final point (γ_n, ϵ) *in the direction of increasing* γ *the solution becomes stable. As* γ *continues to increase the solution branch eventually coalesces with the trivial solution branch.*

The current work merely begins the task of characterizing the global dynamics of the nonlocal equation. We have provided, at best, only numerical evidence for subsets of the attractor. A complete characterization promises to be a very challenging undertaking. These results, however, provide a firm starting point for more in-depth exploration, and the possibilities for continued research appear to be abundant.

One possible direction is to provide rigorous proof of the results of Chapter 5. Even in the limited parameter regime we have considered this promises to be difficult. The inability to make use of classical results such as maximum principles and comparison arguments significantly complicates the problem.

Continuing the numerical characterization into larger regions of parameter space also seems to be a challenging undertaking. This requires approximations of increasingly higher dimension to capture the dynamic behavior and the bifurcation structure has the potential to become rather complex.

Finally, it is still not known whether the heteroclinic connections we have found for the nonlocal equation perturb to connections for the system

$$\frac{du}{dt} = \epsilon^2 u_{xx} + f(u) - w, \quad u_x(0,t) = u_x(1,t) = 0 \tag{6.1}$$

$$\delta \frac{dw}{dt} = w_{xx} + \gamma u - w, \quad w_x(0,t) = w_x(1,t) = 0. \tag{6.2}$$

The geometric singular perturbation theory for infinite-dimensional equations is still in its infancy and there are presently very few results. A natural continuation of the analysis we have completed here seems to be the numerical verification that the connections do indeed perturb.

REFERENCES CITED

[1] R. A. Adams. *Sobolev Spaces.* Academic Press, New York, 1975.

[2] F. Bai, A. Spence, and A. M. Stuart. The numerical computation of heteroclinic connections in systems of gradient partial differential equations. *SIAM Journal on Applied Mathematics*, 53:743–769, 1993.

[3] S. Chow and J. Hale. *Methods of Bifurcation Theory.* Springer Verlag, New York, 1982.

[4] S. Chow and K. Lu. Invariant manifolds for flows in Banach spaces. *Journal of Differential Equations*, 74:285–317, 1988.

[5] E. Conway, D. Hoff, and J. Smoller. Large time behavior of solutions of systems of nonlinear reaction-diffusion equations. *SIAM Journal on Applied Mathematics*, 35:1–16, 1978.

[6] M. G. Crandall and P. H. Rabinowitz. Bifurcations from simple eigenvalues. *Journal of Functional Analysis*, 8:321–340, 1971.

[7] L. Debnath and P. Mikusinski. *Introduction to Hilbert Spaces with Applications.* Academic Press, New York, 1990.

[8] E. J. Doedel. Auto: A program for the automatic bifurcation and analysis of autonomous systems. In *Proc. 10th Manitoba Conference on Numerical Mathematics and Computing*, pages 265–282, 1981.

[9] N. Dunford and J. T. Schwartz. *Linear Operators Part II: Spectral Theory.* Interscience Publishers, New York, 1963.

[10] L. Edelstein-Keshet. *Mathematical Models in Biology.* The Random House/Birkhauser Mathematics Series, 1987.

[11] P. C. Fife. *Dynamics of Inernal Layers and Diffusive Interfaces.* Society for Industrial and Applied Mathematics, Philadelphia, 1988.

[12] C. Foias, G. R. Sell, and R. Temam. Inertial manifolds for nonlinear evolution equations. *Journal of Differential Equations*, 73:309–353, 1988.

[13] M. Golubitsky and D. Schaeffer. *Singularities and Groups in Bifurcation Theory.* Springer-Verlag, New York, 1984.

[14] J. Hale. *Asymptotic Behavior of Dissipative Systems: AMS Mathematical Surveys and Monographs Number 25.* American Mathematical Society, Providence, 1988.

[15] J. Hale and K. Sakamoto. Shadow systems and attractors in reaction-diffusion equations. *Applicable Analysis*, 32:287–303, 1989.

[16] D. Henry. *Geometric Theory of Semilinear Parabolic Equations: Lecture Notes in Mathematics Vol. 840.* Springer-Verlag, Berlin, 1981.

[17] The Mathworks Inc. *MATLAB 4.2: High Performance Numeric Computation and Visualization Software.* Natick, MA, 1994.

[18] M. S. Jolly. Explicit construction of an inertial manifold for a reaction-diffusion equation. *Journal of Differential Equations*, 78:220–261, 1989.

[19] M. S. Jolly, I. G. Kevrekidis, and E. S. Titi. Approximate inertial manifolds for the Kuramoto-Sivashinsky equation: Analysis and computations. *Physica D*, 44:38–60, 1990.

[20] J. P. Keener. Secondary bifurcations in nonlinear diffusion reaction equations. *Studies In Applied Mathematics*, 55:187–211, 1976.

[21] M. Marion. Approximate inertial manifolds for reaction diffusion equations in high space dimension. *Journal of Dynamics and Differential Equations*, 1:245–265, 1989.

[22] J. Murray. *Mathematical Biology.* Springer-Verlag, Berlin, 1986.

[23] Y. Nishiura and H. Fuji. Stability of singularly perturbed solutions to systems of reaction-diffusion equations. *SIAM Journal of Mathematical Analysis*, 18:1726–1770, 1987.

[24] Y. Nishiura and M. Mimura. Layer oscillations in reaction-diffusion systems. *SIAM Journal on Applied Mathematics*, 49:481–514, 1989.

[25] A. Pazy. *Semigroups of Linear Operators and Applications to Partial Differential Equations.* Springer-Verlag, Berlin, 1983.

[26] R. D. Russell, D. M. Sloan, and M. R. Trummer. Some numerical aspects of computing intertial manifolds. *SIAM Journal of Scientific Computing*, 14:19–43, 1993.

[27] K. Sakamoto. Construction and stability analysis of transition layer solutions in reaction-diffusion systems. *Tohoku Math. J.*, 42:417–44, 1990.

[28] J. Smoller. *Shock Waves and Reaction-Diffusion Equations, Second Edition.* Springer-Verlag, Berlin, 1994.

[29] R. Temam. *Infinite Dimensional Dynamical Systems in Mechanics and Physics.* Springer-Verlag, New York, 1988.

[30] A. M. Turing. The chemical basis of morphogenesis. *Philosophical Transactions of the Royal Society of London*, 32:37–72, 1952.

[31] E. Zeidler. *Nonlinear Functional Analysis and its Applications Volume I: Fixed Point Theorems.* Springer-Verlag, New York, 1986.

MONTANA STATE UNIVERSITY LIBRARIES
3 1762 10293262 9